Journal of Fluorescence (2020) 30:1295–1330
https://doi.org/10.1007/s10895-020-02554-7

REVIEW

A Mini Review on Organic Chemosensors for Cation Recognition (2013-19)

Nilima S. Patil[1,2] · R. B. Dhake[1] · Mohd Imran Ahamed[3] · Umesh Fegade[2]

Received: 16 February 2020 / Accepted: 11 May 2020 / Published online: 15 September 2020

Abstract

Colorimetric and ratiometric fluorescent probe for cations gain very well attention by the chemist, biologist and environmentalist. Metals has two sides, first is biolgical active for living creature and toxic nature for the ecosystem. From last three decades the scientists are contiously trying to find out the best solution for the detection of cations at micro as well as nanomolar levels. In the present review we discussed the colorimetric and ratiometric fluorescent probe synthesized by the authors in almost half decade.

Keywords Colorimetric · Fluorescent probe · Biolgical active · Nanomolar levels

Abbreviations

DNA	Deoxyribonucleic acid
RNA	Ribonucleic acid
F-AAS	Flame Atomic absorption spectrometry
ICP	inductively coupled plasma
CT	Charge Transfer
LOD	Limit of detection
K_b	Bindig constant
ET	Electron Transfer
FRET	Förster Resonance Energy Transfer
K_a	Association constant
K_s	Stability constant
CH_3CN	Acetonitrile
CH_3OH	Methanol
C_2H_5OH	Ethanol
HRMS	High rsolution mass spectroscopy
PBS buffer	Phosphate-buffered saline buffer
μM	micro molar
DFT	Density functional theory
mM	Mili molar
ICT	Intramolecular charge transfer
DMSO	Dimethyl sulfoxide
B-H	Benesi-Hildebrand
S-P	Scatchard-plot
PET	Photo electron effect
HOMO	Highest occupied molecule orbital
LUMO	Lowest unoccupied molecular orbital
FMO	Frontier molecular orbitals
GNs	Graphene nanosheets
CAN	Acetonitrile
CTAC	Cetyltrimethylammonium chloride
DSSC	Dye-sensitized solar cell
CHEF	Chelation-enhanced fluorescence

✉ R. B. Dhake
drrbdhake@gmail.com

✉ Umesh Fegade
umeshfegade@gmail.com

1 Department of Chemistry, D. N. Bhole College, Bhusawal 425201, MH, India

2 Department of Chemistry, Bhusawal Arts, Science and P. O. Nahata Commerce College, MH Bhusawal 425201, India

3 Department of Chemistry, Faculty of Science, Aligarh Muslim University, Aligarh 202 002, India

Introduction

Sensing of cations is gaing more attention by many scientists, including chemists, biologists, and environmentalists. Metals are involved in many vital biological course of action such as transmission, muscle contraction, cell activity, etc. [1–5]. Metals play a crucial role in cell functions. It is involved in electron transfer processes in DNA and RNA synthesis by facile redox chemistry and its high affinity for oxygen [6–13].

Several methods such as F-AAS, AAS, ICP emission spectrometry, spectrophotometry, voltammetry and electrochemical stripping analysis have been developed for detecting metal ions [14–20]. Conventional process has good accuracy but needed expensive instrument and tedious process for detection, and very less applicability in situ analysis [21–26]. UV–visible and fluorescence spectroscopy is most favorable modes over other common technique for the detection of environmental significant samples because its concentration is very less in nature [27–31].

Among various photophysical pathways like Charge Transfer (CT), Electron Transfer (ET), Förster Resonance Energy Transfer (FRET), are generally utilized for reporting the binding induced phenomena [32–39]. In last few decates, many authors sythesise the sensor for the sensing of metal ions and susesfully reported its biological application.

Need for Chemosensors

In the last few decades, the awareness regarding the significance and toxic effect of cation is well understood by the scientist in the field of chemistry, biology and environment [40–42]. Various heavy metal ions uses are banned by various international agencies, because of its toxic nature, nonbiodegradable and hence can accumulate in the environment and foodchain [43–49].

Today, scientist and chemist are trying to develop a cation chemical sensor which can be used for analysis of environmental sample and industrial sample. On the other hand the biosensor is used in medicine and biological application.

Chemosensors for Cations

1 was developed by pyridine-2-hydrozine which shows 7.63-fold fluorescent enhancement for Zn^{2+} in CH_3CN/HEPES(*v/v* 1:1) [50]. 1:1 complexation formation supported using HRMS. The association constant $1.83 \times 10^5 M^{-1}$ and LOD for Zn^{2+} ion 2.2×10^{-6}M and effectively useful in the cell-imaging of Zn^{2+}. 2-((benzylimino)-methyl)-naphthalen-1-ol (**2**) shows discraminating emmision for Cu^{2+} and Zn^{2+} under ACN [51]. The binding constant for Cu^{2+} and Zn^{2+} $(6.55 \pm 0.8) \times 10^3\ M^{-1}$ and $(4.32 \pm 0.8) \times 10^4 M^{-1}$ respectively and free energy change calculated -26.44 kJmol^{-1} for Zn^{2+} and -21.77 kJmol^{-1} for Cu^{2+}, negative free energy indictates the thermodynamic feasibility. Probe **3** [52] selective for Au^{3+} by discriminant colour transform from yellow-to-pink in PBS 4% ethanol pH = 7.4 (Fig. 1**)**. The LOD was determined to be 8.44×10^{-6}M and cell imaging response rates of **3** to Au^{3+} in differentiated adipocytes are greater than HeLa cells, because lipid droplets in adipocytes act as surfactants.

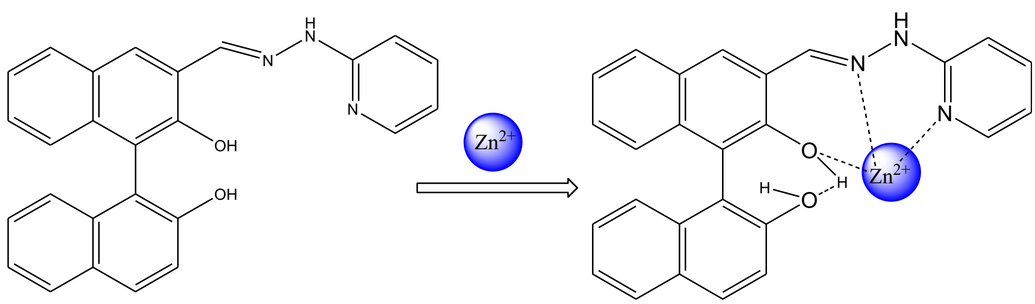

1

1.Zn^{2+}

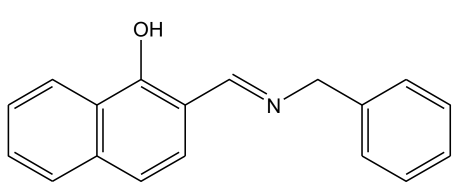

2

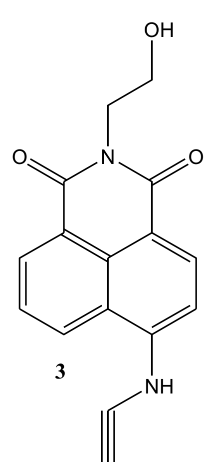

3

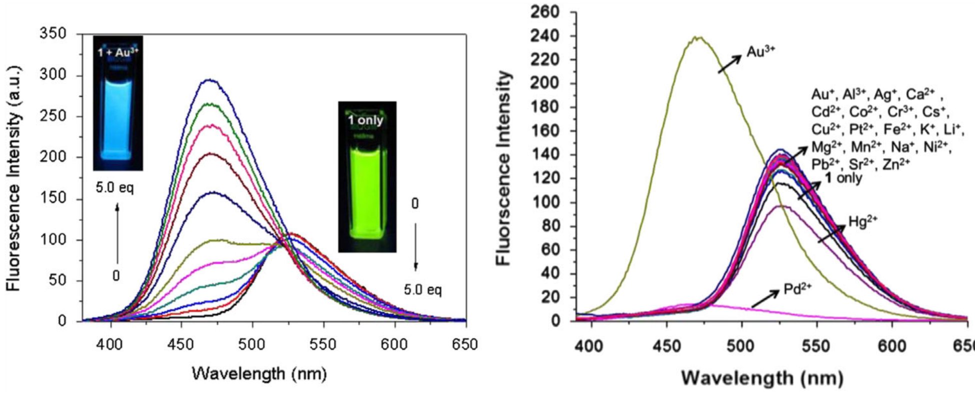

Fig. 1 Left: Au^{3+} ion-induced (0, 0.2, 0.4, 0.6, 0.8, 1.0, 1.5, 2.0, 3.0, 4.0, 5.0 equiv) changes in the fluorescence spectrum of **3** (20 μM) in PBS buffer containing 4% ethanol at pH 7.4 in the presence of CTAC (50 μM). Right: Fluorescence response of **3** (20 μM) to various metal ions (5 equiv) in PBS buffer containing 4% ethanol at pH 7.4 in the presence of CTAC (50 μM). All the fluorescence data were obtained after 60 min incubation of **3** with metal ions ($\lambda_{ex} = 364$ nm, slit: 3 nm/3 nm). 'Reprinted from reference number 52 with permission of Elsevier publication'

4a and **4b** [53] absorption data shows a yellow solution to orange-red solution on Hg^{2+} ($\lambda_{abs.max} = 506 \rightarrow 532$ nm) addition with "naked eye" detection at concentrations 10^{-6}M. Cellular neurobiological studies were then undertaken extremely low cell toxicity is also evident with this probe. **5a** and **5b** detect Hg^{2+} with change of colour from colourless to pink, visible to the naked eye [54]. The quantum yield for **5a** and **5b** was ($\Phi = 0.004$ and 0.0034), **5a**.Hg^{2+} and **5b**.Hg^{2+} was ($\Phi = 0.68$ and 0.46) and LOD of **5a** and **5b** 50×10^{-9}M and 10×10^{-8}M respectively. Rhodamine-naphthalimide derivative sensor **6** was used for effective sensing of Cu^{2+} with large red shift (115 nm) [55]. The detection limit was 3.88×10^{-7}M for Cu^{2+} and Cytotoxicity testing in MCF-7 cells shows that **6** is almost nontoxic to living cells (Fig. 2).

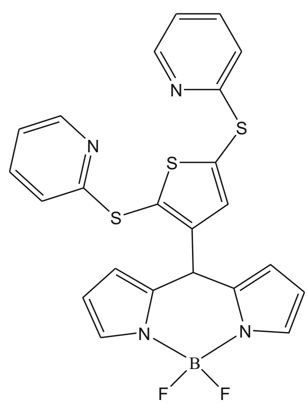

4a

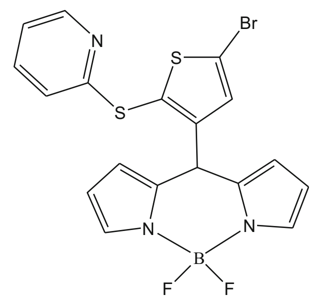

4b

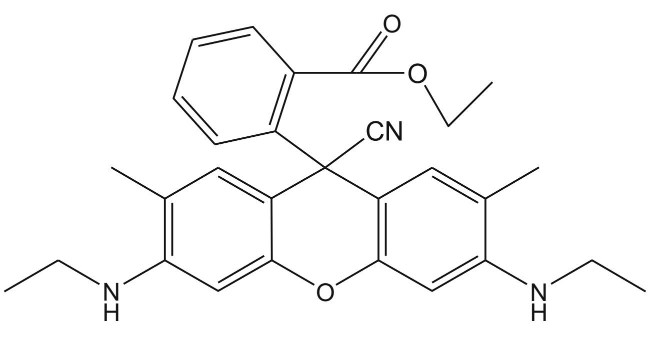

7

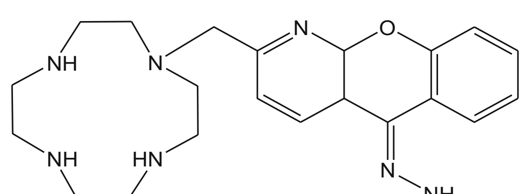

8

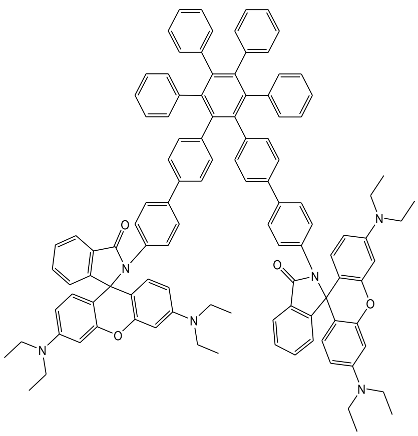

5a

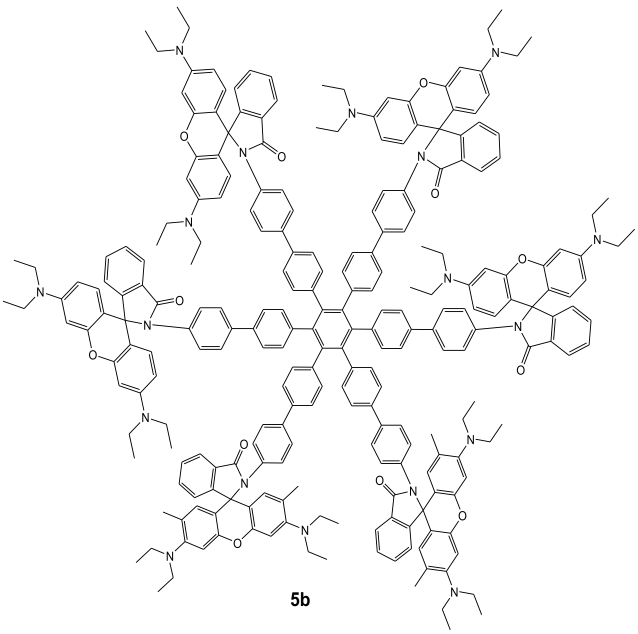

5b

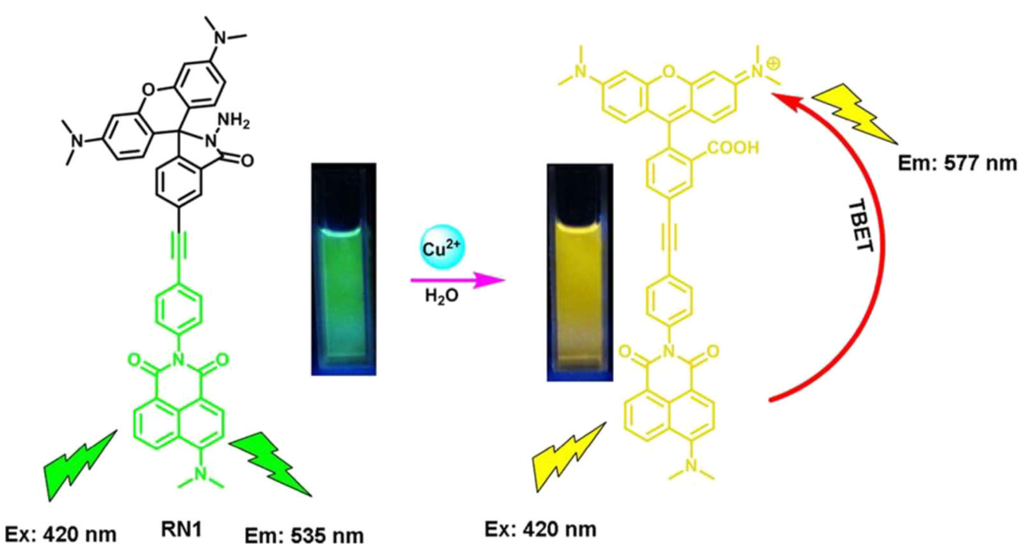

Fig. 2 Sensing mechanism of chemosensor **6** with Cu^{2+} ion. 'Reprinted from reference number 55 with permission of ACS publication'

A cyano-rhodamine moiety **7** easily undergoes selective Pd^{2+} induced 'C–CN' bond breaking to produce the pink coloration of rhodamine with an 88-fold enhancement of quantum yield [56]. Sensor **7** biological applicability shown by the cell imaging of Pd^{2+} on HeLa-cells and LOD of the Pd^{2+} is found to be 0.57 μM. Cyclen based receptor **8** was developed for the

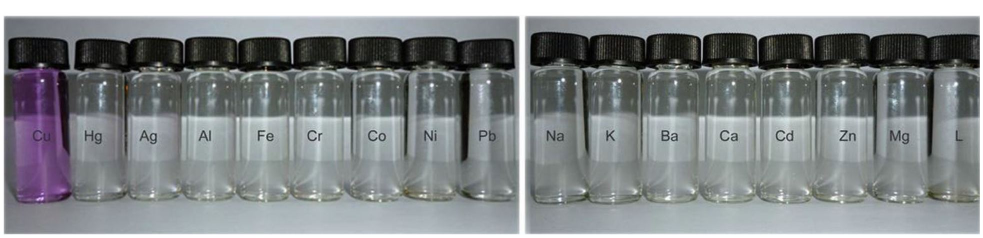

Fig. 3 Change in color of 10 μM **13** in CH_3OH/HEPES (20 mM, pH7.2, 1:1,v/v) semiaqueous solution with 5-time cation from left to right: Cu^{2+}, Hg^{2+}, Ag^{+}, Al^{3+}, Fe^{3+}, Cr^{3+}, Co^{2+}, Ni^{2+}, Pb^{2+}, Na^{+}, K^{+}, Ba^{2+}, ca.$^{2+}$, Cd^{2+}, Zn^{2+}, Mg^{2+} and only **13**. 'Reprinted from reference number 62 with permission of Elsevier publication'

recoginition of Zn(II) with enhancement in fluoresecnec spectra [57]. In MeOH, **8** is poorly fluorescent (ϕ ≈ 0.4%) with addition of Zn^{2+}, the fluorescence increases. Stiochiometric was 1:1 and 2:1 for Zn:**8** complexes. Sikdar and its coauthors [58] synthesised a rhodamine-B-based **9** for detection of Cu^{2+} ion aqueous media and inside living cells. The 1:1 complex is confirmed, bindng constant is found at 2.5×10^4 and LOD at 1.22 μM. Pyrene-based **10** (ϕ ≈ 0.001) was synthesized as Fe^{3+} sensor in biological environment (ϕ ≈ 0.0.041) [59]. The 1:1 stiochiometry **10**.Fe^{3+} is estimated by Job's method and ESI-MS and association constant found to be $1.27 \times 10^4 M^{-1}$.

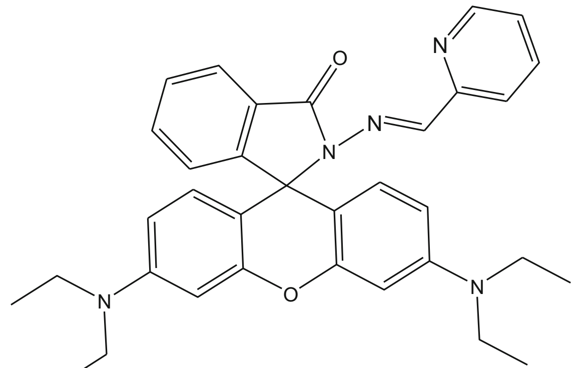

9

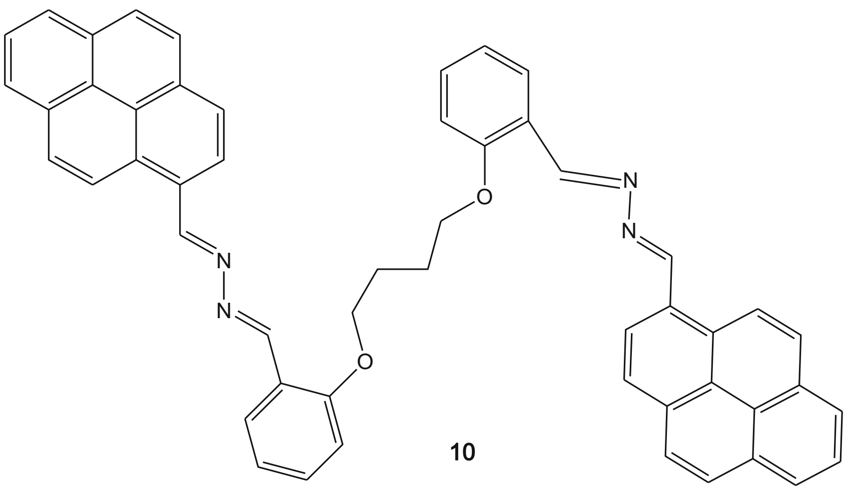

10

Wang et al. [60] synthesized **11** for Zn^{2+} sensing, with red fluorescence in methanol ($\lambda_{em} \approx 630$ nm, $\Phi_{fl.} \approx 0.8$). A probe **12** based on 2,2′,6′,2″-terpyridine for the detection of Zn^{2+} (green) and Cd^{2+} (blue) [61]. The association constants (log K_a) of the probe **12** for Zn^{2+} and Cd^{2+} are found to be 3.75 and 3.62 respectively. The detection limit of **12** for Zn^{2+} and Cd^{2+} found to be 1.63 and 2.81 ppb respectively. Probe **13** shows colorimetric colour [62] and significant enhancment in absorbance (Fig. 3) change on the micromolar level addition of Cu^{2+} and the LOD at $7.27 \times 10^{-7} M^{-1}$.

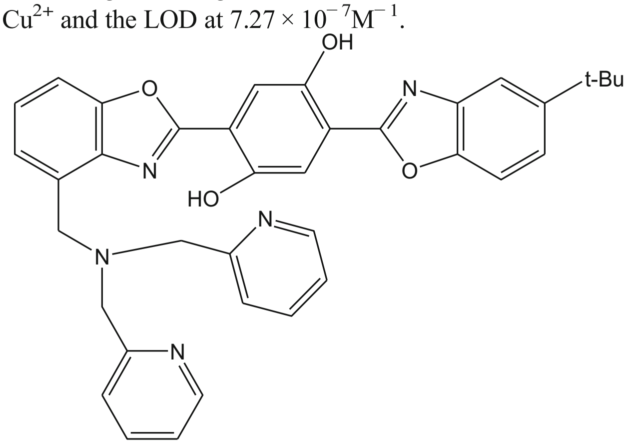

11

Chawla et al.. synthesized **14** a calix[4]arene derivatives used for the detection of Cu^{2+} [63]. Analysis of the data obtained from Job's-plot revealed the 1:1 molecular complexation. A peak at m/z 1170.5413 in ESI-MS data showed the formation of 1:1 complex $[8 + Cu^{2+} + ClO_4]^+$. The detection limit was found to be 6.02×10^{-6}M and association constant, value $1.655 \times 10^6 M^{-1}$. Kuwar et al.. synthesized sensor **15** characterized by X-ray crystallography and explore its sensing ability towards Cu^{2+} [64]. 1:1 stoichiometry formed between **15** and Cu^{2+} and association constant calculated by B-H and S-P at $(43000 \pm 11) M^{-1}$. Probe **16** based on 1,8-naphthalimide and rhodamine shows green-to-orange transformation with addition of Cr^{3+} in CH_3CN–HEPES buffer solution. The LOD found to be at 0.14 nM and 1:2 complexation. **16** is successfully applied to detect Cr^{3+} in cell lysate and blood serum [65]. Chereddy et al.. synthesized the naphthalimide based probe (**17**) which demonstrated high emission intensity upon Fe^{3+} addition [66]. The binding constants and LOD were found to be $1.04 \times 10^5 M^{-1}$ and 3.0×10^{-8}M, respectively. The **17** is stable, nontoxic and 'turn-on' for the imaging of intracellular Fe^{3+} ions.

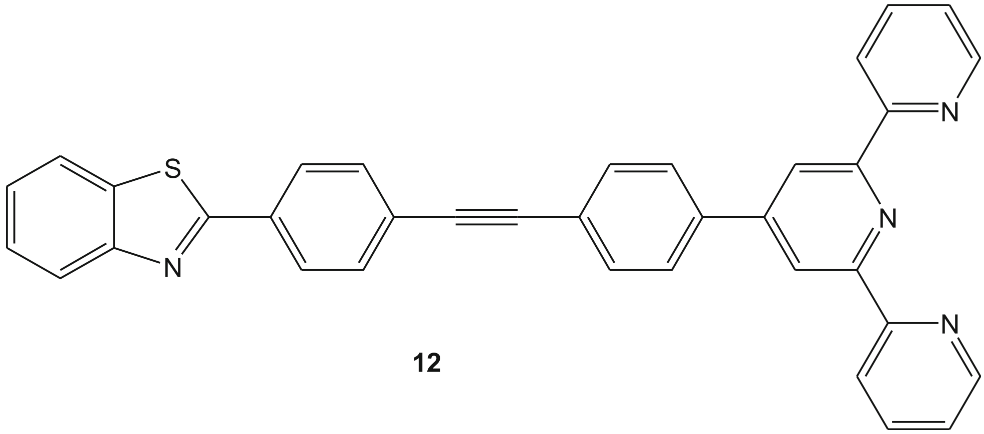

12

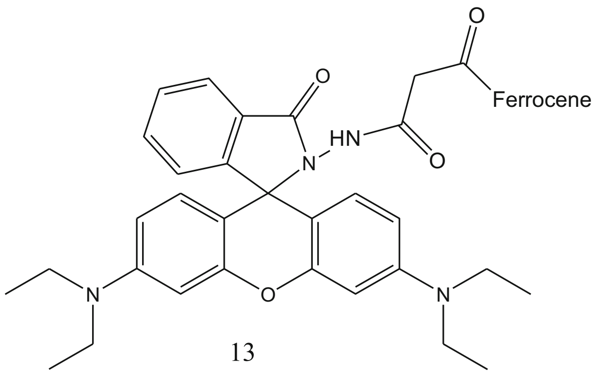

13

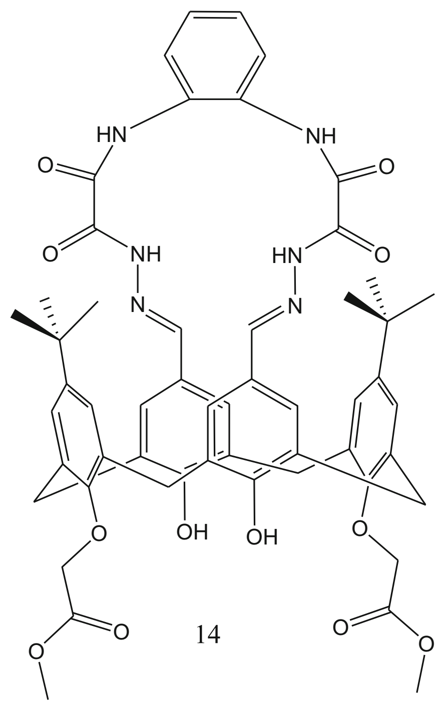

14

A TACN (1,4,7-triazacyclononane) derivatives of **18a** and **18b** which has ability to recognize the zinc ion [67]. The fluorescence quantum yield of **18a**-Zn (ϕ = 0.070) is 2.6-fold greater than free 5 (ϕ = 0.027), and more than twice that of **18b**-Zn (ϕ = 0.032) with 1:1 complexation. A 5-diethylamino-2-(quinolin-8-yliminomethyl)-Phenol probe (**19**) which is capable of detecting multiple ions, Mg^{2+} and Zn^{2+}, fluorescence and Co^{2+} by UV/Vis [68]. The LOD for Mg^{2+} and Zn^{2+} was 70 nM and1.85 μM. The binding constant for the complex of Mg^{2+}, Zn^{2+} and Co^{2+} was calculated to be $8.17 \times 10^6 M^{-2}$, $1.03 \times 10^6 M^{-2}$ and $1.78 \times 10^{22} M^{-2}$ respectively. Hu et al.. [69] developed a sensor **20** for the effective sensing of Hg^{2+} with limit of detection very low at 9.56×10^{-9}M and furthermore it is used as test kit for Hg^{2+} sensing. In ^{1}H-NMR titration experiments chemical shifts of NH appearing at a low-field of the probe **20** at 13.21 ppm, and led to the sensor **20** of the conjugate rigid plane structure.

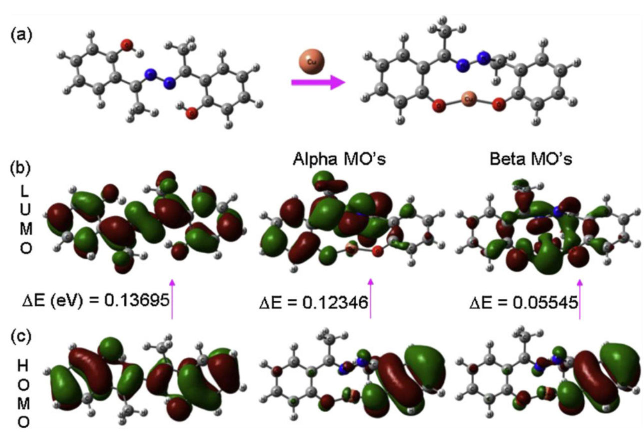

Fig. 4 **a** Receptor **21** and **21**.Cu^{2+}, **b** LUMO, **c** HOMO of **21** and **21** − Cu^{2+} complex. 'Reprinted from reference number 70 with permission of Elsevier publication'

Fegade et al. developed probe **21** for selective detection of Cu^{2+} [70]. DFT indicates **21**:Cu^{2+} showed the ICT, lesser the band-gap between the HOMO-LUMO of **21** which due to change in spectra (Fig. 4**)**. The LOD was calculated at 50 nM and K_b at 11667M^{-1}. Rhodamine-B derivative probe **22** is colorimetric and fluorescent naked eye sensor for Hg^{2+} [71]. Quantum yield of **22** was < 0.05%, quantum yield of **22**-Hg^{2+} was found to be 14.6%. The stoichiometric ratio is 1:3 and LOD found to be 0.75 ppb. A PET fluorescence chemodosimeter **23** was designed for Cu^{2+} detection [72]. Upon addition of Cu^{2+}, **23** solution changed from pink to green and acts as a colorimetric chemodosimeter. The 1:1 stoichiometry estimated by Job's plot and the LOD at 2.3×10^{-7}M. Roy et al.. [73] synthesized probe N,N/-bis(salicylidene)trans1,2–diaminocyclohexane (**24**) has chemoselective Zn^{2+} sensor. The quantum yield increases drastically from 3.6×10^{-3} for **24** compared to 1.8×10^{-1} for **24**–Zn^{2+} complex. 1:1 complexation estimated by continous variation method and the K_a was at $3.7 \times 10^4 M^{-1}$. Rhodamine-B derivative sensor **25** was developed, which exhibits effective sensing for Hg^{2+} in ethanol solution [74]. 1:1 stoichiometry estimated by Job's plot and LOD at 3.1×10^{-6}M. The filter paper in the present Cu^{2+} or Hg^{2+} showed a pink color change, only Hg^{2+} induced a strong yellow color change under UV lamp.

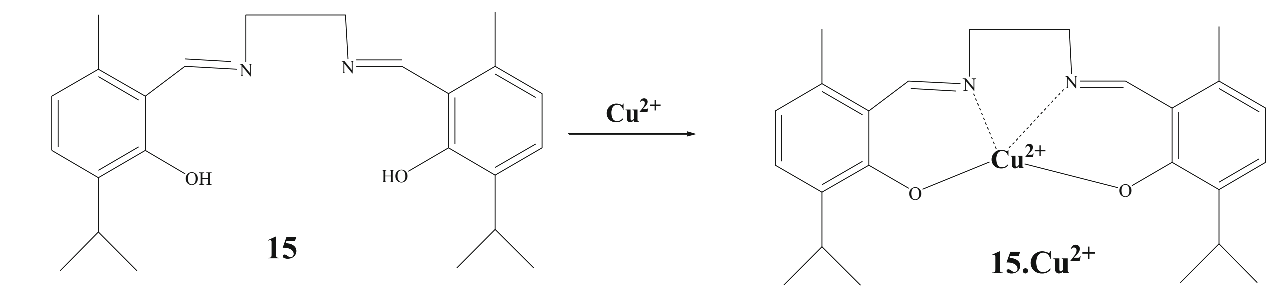

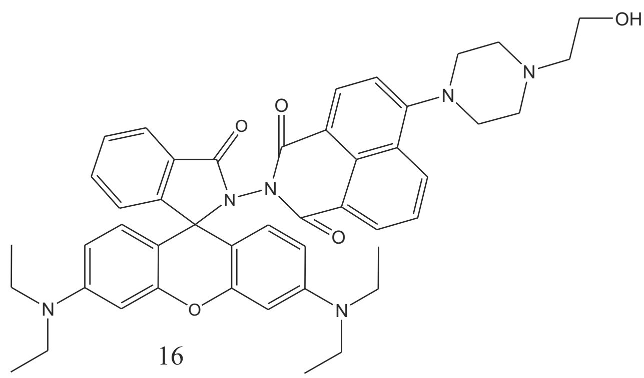

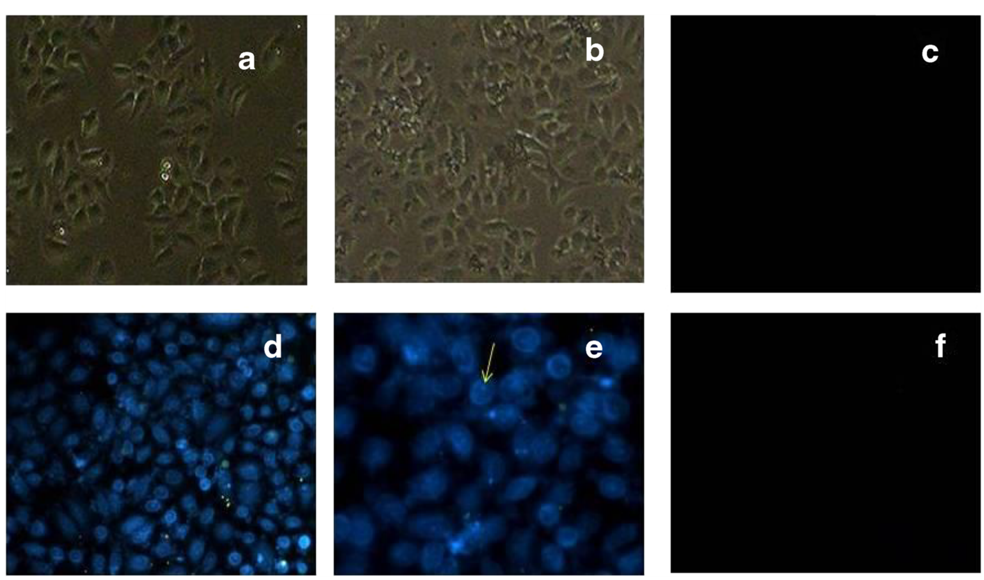

Fig. 5 **A** Control cells devoid of receptor **30** and Zn^{2+}, **B** HeLa cells with receptor **30**, **C** Fluorescence image with only receptor **30**, **D** Fluorescence image with receptor **30** and Zn^{2+}, **E** In higher magnification uptake of Zn^{2+} is visible [arrow head]. **F** Fluorescence image with only Zn. 'Reprinted from reference number 79 with permission of Elsevier publication'

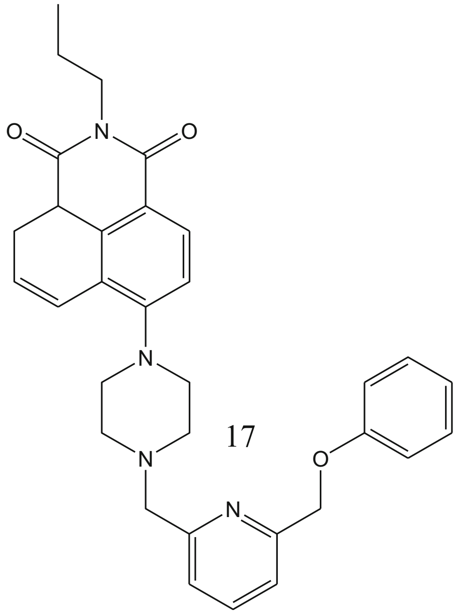

17

Probe **26**, can selectively detect Co^{2+} in CH_3OH/H_2O (70:30,v/v) solution [75]. DFT study shows the tautomeric form of **26** found to be less stable by 11.37kcalmol^{-1} and **26**.Co^{2+} lowering of energy by -358.88kcalmol^{-1} which indicates stable Complex. 1:1 complexation was determined using continous variation method and K_s at 50000M^{-1}. **27** exhibited a remarkable selectivity for Zn^{2+} and its absorbance at 256 nm gradually increased with addition of Zn^{2+}. Fluorescence emission of **27** exhibits at 408 nm with $\Phi = 0.069$ and with the addition of Zn^{2+} the 81 nm red-shift from 408 to 489 nm with $\Phi = 0.138$. DFT shows the HOMO–LUMO energy gap for the **27**–Zn complex (3.34 eV) is smaller than **27** (4.20 eV) [76]. Zhang et al. [77] developed chemosensor (**28**) for selective detection of Hg^{2+}. In the UV-vis spectrum of **28** shows broad absorption from 405 to 490 nm vanished when Hg^{2+} were added. **28** emitted very weakly ($\lambda_{em} = 428$ nm; $\lambda_{ex} = 345$ nm), demonstrating that the predictable fluorescence of the naphthalene units was quenched via transformation in ICT state. A probe, (E)-3-(3-(4-([2,2':6',2''-terpyridin]-4'-yl)phenyl)acryloyl)-7-(diethylamino)-2H-chromen-2-one (**29**), used for sensing of Zn^{2+} with low LOD at 10 nM and also shows imaging of Zn^{2+} in cells as applications in cell-imaging [78]. DFT shows when Zn^{2+} coordinated with the **29**, the electrons are located on the coumarin part in the ground state, but are rearranged to the part from carbonyl to the terpyridine group when excited, showing ICT effect. **30** had a high affinity and selectivity towards Zn^{2+} and shows detection of Zn^{2+} in intracellular environment of HeLa cell [79]. The detection limit for Zn^2 at 35 nM and binding constant K_a was about $(2.1 \pm 0.3) \times 10^5 M^{-1}$ (Fig. 5).

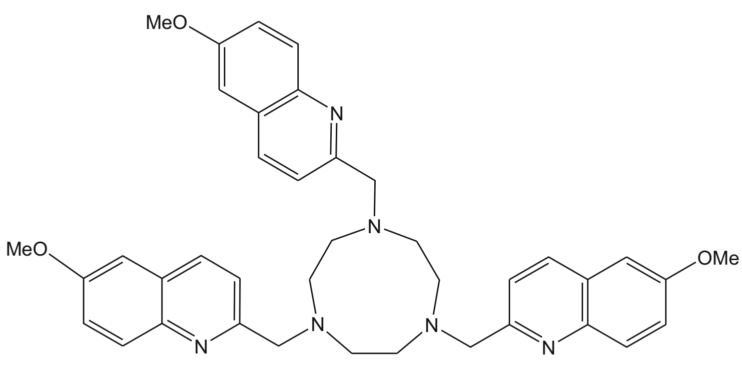

18a

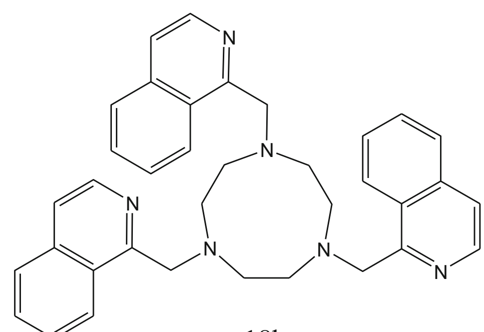

18b

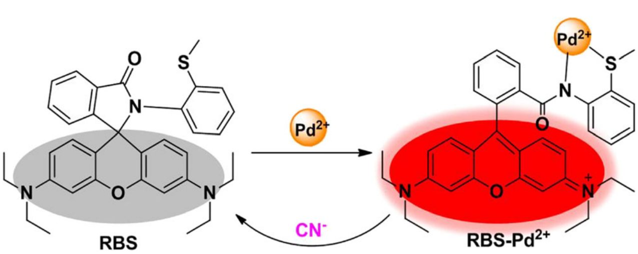

Fig. 6 Proposed Mechanism for the Identification of Pd^{2+} by **31**. 'Reprinted from reference number 80 with permission of ACS publication'

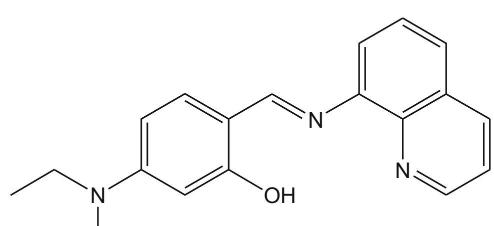

19

Mian Wang et al. synthesized "turn-on" chemosensor (**31**) for Pd^{2+} [80] with LOD calculated at 2.4 nM. 1:1. Job-plot and HRMS provided evidence for the formation of a 1:1complex of **31**-Pd^{2+} (Figs. 6 and 7). Probe **32** demonstrated high selectivity by discriminating Al^{3+} over other metal ions and LOD at 21.6 nM [81]. Furthermore, to check its biocompatibility sensing of Al^{3+} has been done in live cells. Azodye–rhodamine based probe (**33**) has been designed [82] for selective detection of Pd^{2+} with 40-times increses in fluorescence by red-shift. The 1:1 stoichiometry determined by Job's plot and LOD 0.45 μM at pH 7.4. Furthermore, the probe **33** used to image Pd^{2+} in living cells. A reversible fluorescent-colorimetric imino-pyridyl bis-Schiff base receptor **34** (N1E,N4E)-N1,N4-bis(pyridine-4-ylmethylene)benzene-1,4-diamine for the detection of Al^{3+} in aqueous medium [83]. The LOD at 0.903 μM for Al^{3+} is very low than the limit recommended by WHO (7.41 μM). ^{1}H-NMR titration and MASS shows that the formation of 1:2 complexation. Zhiyuan Zhang et al. synthesised probe **35** and used for the effective detection of Cr^{4+}[84]. The sensing mechanism was explored by reversibility and LC/MS, and the results suggested that the recognition was based on the oxidation of the primary alcohol in the structure of the sensor by the Cr^{4+} sources.

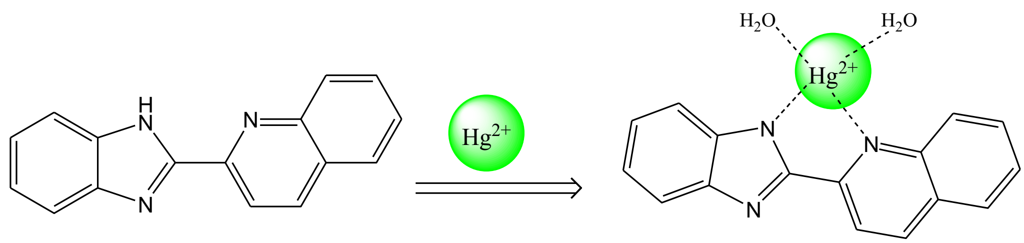

20

20.Hg Complex

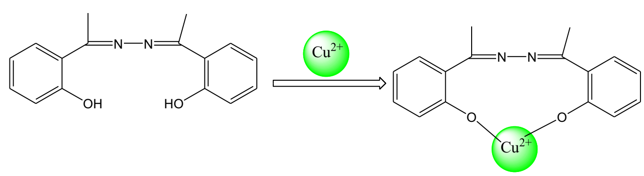

21

21.Cu Complex

Yan-Cheng Wu et al. synthesized three bisbenzimidazole derivatives **36** (Fig. 8) as dual-functional fluorescent and visual sensors for effective sensing of Ag(I) and Fe(III) with a response time of 10 s and steadily work in wide pH 4–13 range. [85]. Jitendra Bhosale et al. explored the selctive sensing of Zn^{2+} cation by pyrrole-based derivative **37** [86]. The sensing behaviour has been supported by UV-vis absorption and DFT calculations indicating the formation of a 1:1 complex between the pyrrole based receptor **37** and Zn^{2+}. The asprepared **37** was further used for cell-imaging. A phthalazine based sensor **38** was designed for sensitive detection of Co^{2+} in CH_3CN–H_2O with LOD at 25 nM. Sensor **38** show that change in colour from yellow to green with red-shifted from 383 nm to 435 nm in the presence of Co^{2+} [87]. The sensor **38** has capability to monitoring Co^{2+} in cell-imaging. Rahul Patil et al. developed probe 3-((2-(1H-benzo[d]imidazol-2-yl)phenylimino)methyl)benzene-1,2-diol (**39**) for selective sensing of Hg^{2+} with LOD low at 0.20 mM [88]. The emission spectrum of probe 39 was quenched on complexation with Hg^{2+} ion. Chemosensor, 2-((E)-(-2-aminophenylimino)methyl)-6-isopropyl-3-methylphenol (**40**), has been designed and confirmed by the single crystal X-ray [89]. The binding constant values for Ni^{2+} and Cu^{2+} were calculated to be 25000 and 30000M^{-1} and detection limits of Ni^{2+} and Cu^{2+} were 100 and 50 nM.

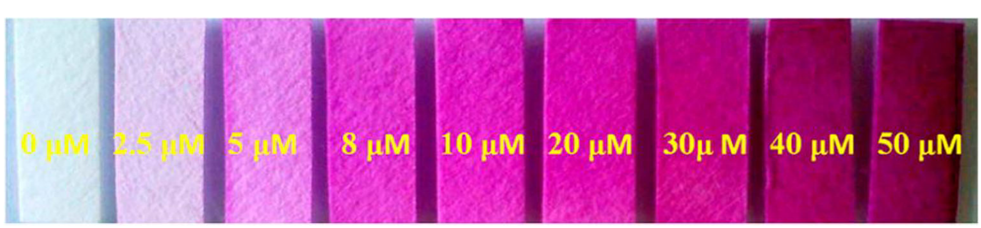

Fig. 7 Colorimetric detection of Pd^{2+} by **31** test paper. 'Reprinted from reference number 80 with permission of ACS publication'

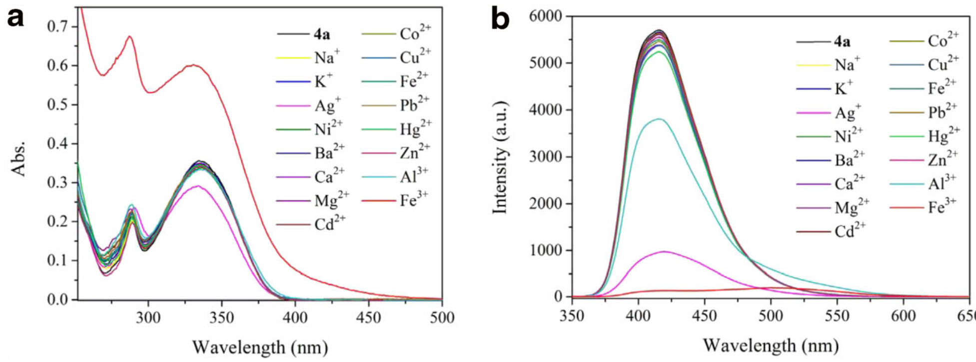

Fig. 8 **a** Ultra violet – visible spectra of **36** adding up of sixteen time of Fe(III) and hundred time of further ions. **b** Emmision of **36** existence of hundred time ions

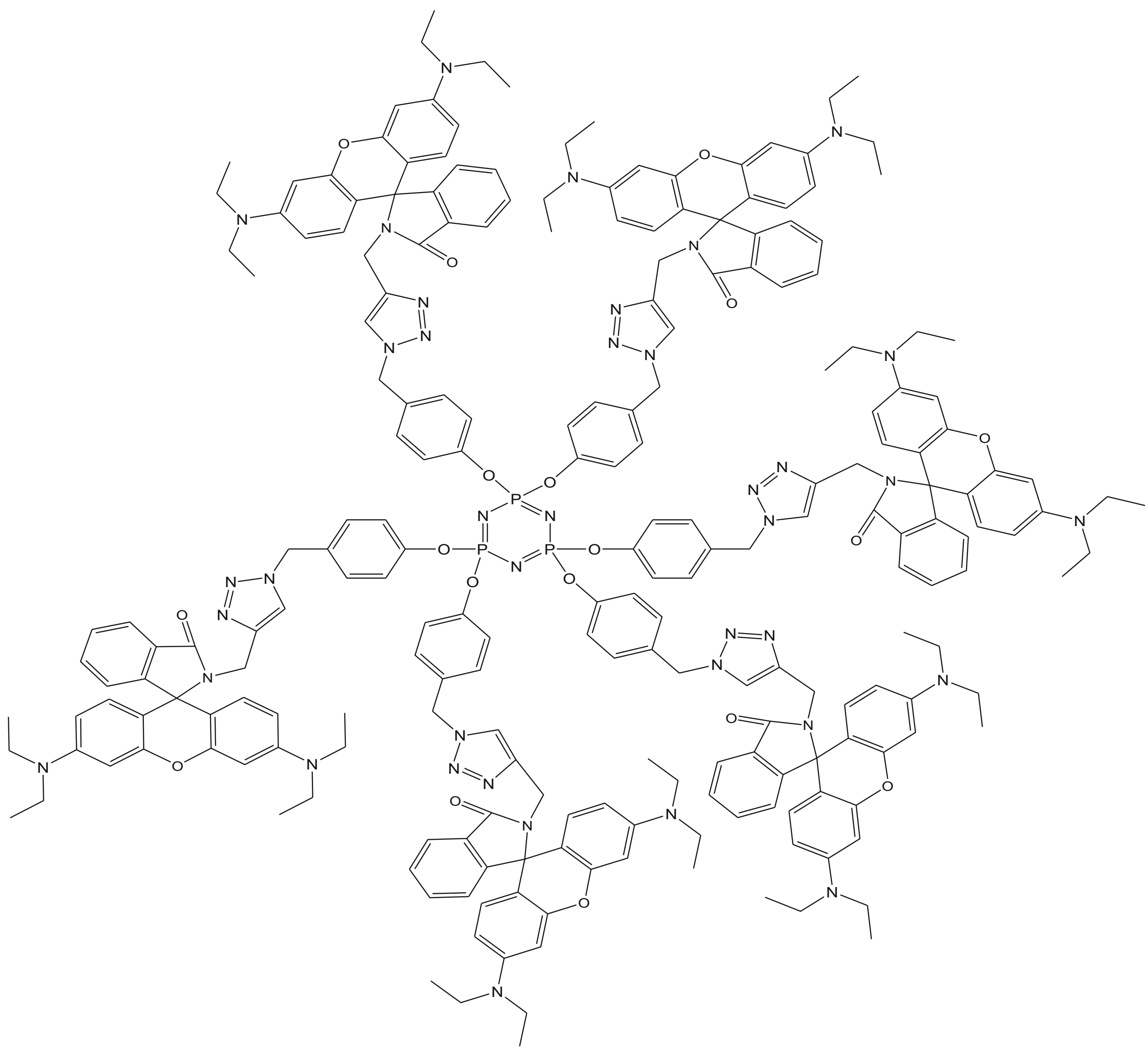

22

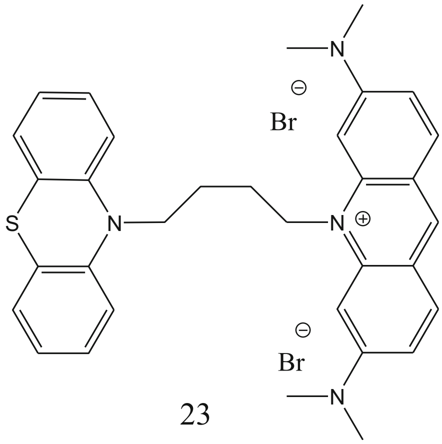

23

Fluorescent receptor (**41**) was designed for the detection of Cu^{2+} and Zn^{2+} with 1:1 complexation and LOD at 5 nM and 15 nM for Cu^{2+} and Zn^{2+} ions, respectively. [90]. Furthermore, it is used as INHIBIT type logic gate at molecular level (Fig. 9). Di Zhou et al. synthesized highly selective fluorescent chemosensor for aluminum(III) ions in DMF [91]. The outcome of ^{1}H-NMR titration, HRMS and density functional theory shows that **42-Al^{3+}** form a 1:1 complexation. The K_a was calculated at 2.67 × 10^6 and the LOD was found at 10^{-6}M. Jie Cui et al. designed a fluorescent probe **43** which has selective recoginition ability for Pd^{2+} which have 21.3 nM LOD [92]. A selective fluorescent sensor **44** based on a pyrazoline derivate was synthesized and applied for the detection of Al^{3+} ion with 1:1 complexation via fluorescent quenching [93]. The K_a value obtained at 1.75 × 10^5M^{-1} and LOD found to be 2.27 × 10^{-7}M.

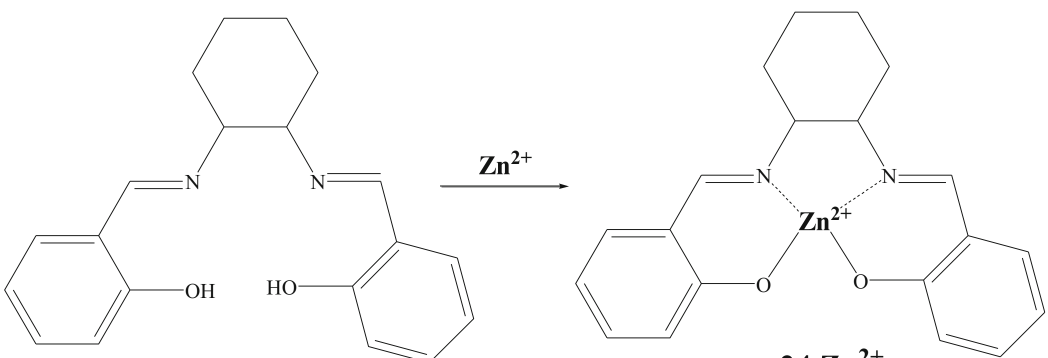

24 **24.Zn^{2+}**

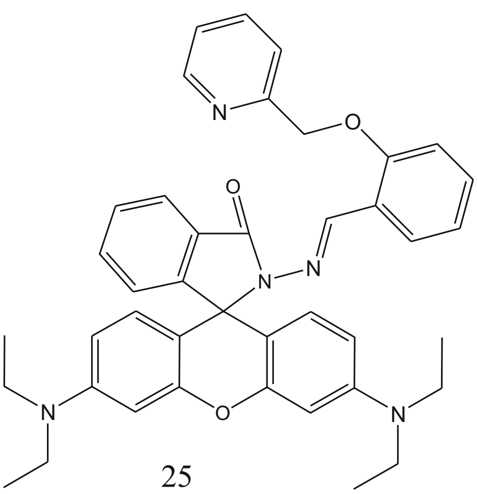

25

Lianqing Li et al. successfully developed a rhodamine derivative chemodosimeter which shows naked-eye fluorescent in the presence of Pd^{2+} [94] (Fig. 10). The detection limit of **45** at 10^{-7}M level and H-G ratio was found at 1:2 according via continuous variation jobs method. Rhodamine functionalized fluorogenic Schiff base **46** was synthesized [95] It exhibited highly selective colorimetric and "off-on" fluorescence response towards Al^{3+}. K_b and LOD of Al^{3+} to **46** are calculated at 1.0 × 10^4M^{-1} and 1.4 × 10^{-7}M, respectively. Berberine (**47**), an important medicinal herb which effectively utilized as a sensing probe for silver ion [96]. The **47** is found to be selective towards Ag + with a detection limit of 0.1 × 10^{-4} molL^{-1}. The effective quenching of **47** uponbinding with Ag^+ ion is attributed to suppression of intramolecular charge transfer (ICT). Quinoline-base sensor **48** showed a highly selective fluorescent enhancement towards Mg^{2+}[97]. The association constant of a 1:1 complex was determined as 1.91 × 10^7M^{-1} and the detection limit was determined as 19.1 ppb. Ahmadreza Bekhradnia et al. reported nitro-3-carboxamide coumarin derivatives (**49**), fopr selective sensing of Cu^{2+} in (HEPES:DMSO) 9:1,v/v) solution [98]. The emmision of 6-nitro-N-[2-(dimethylamino)ethyl]-2-oxo-2H-chromene-3-carboxamide enlarged on the adding up Cu^{2+} with stronger excitation at k = 320 nm than for the other cations tested.

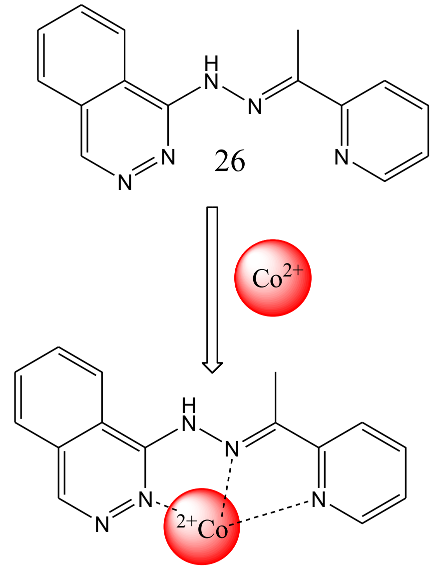

26

26+.Co Complex

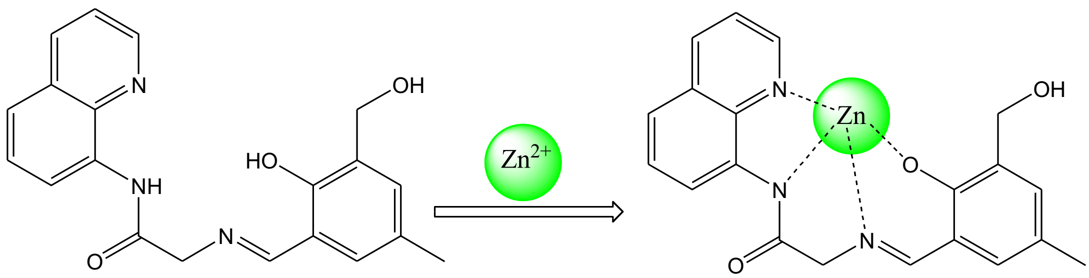

27

27.Zn Complex

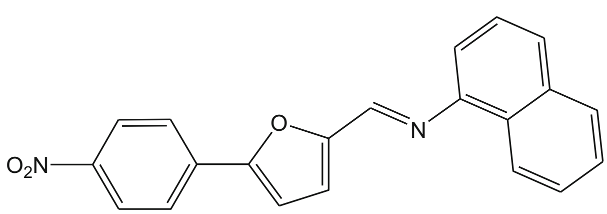

28

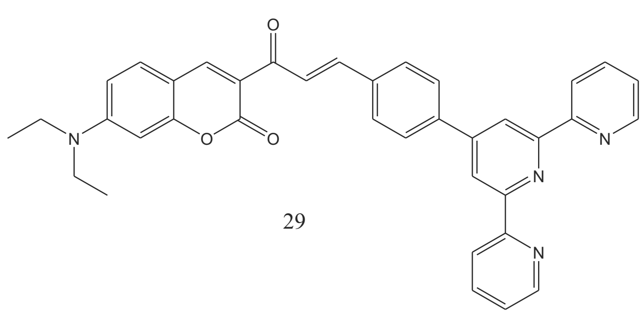

29

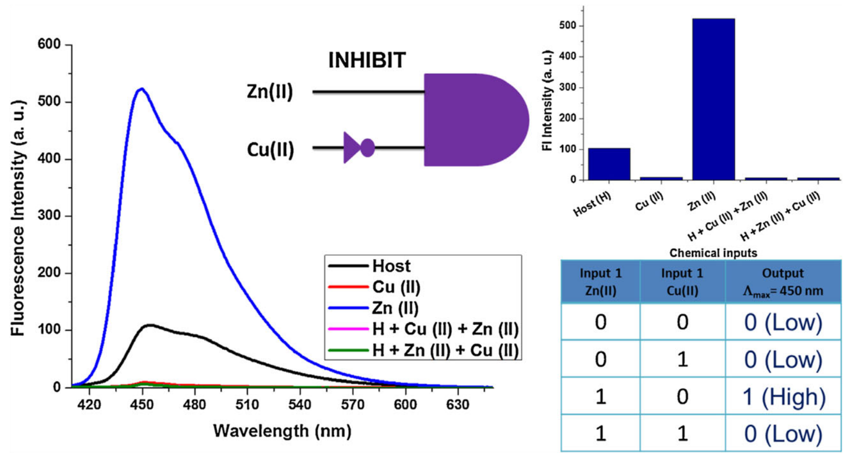

Fig. 9 **A** The changes in the fluorescence spectrum of receptor **41** and **B** the fluorescence intensity at 450 nm in the absence and presence of Zn(II) and Cu(II) for the fabrication of inhibit gate. 'Reprinted from reference number 90 with permission of Elsevier publication'

A dye **50** (Fig. 11) is found to be highly specific in detecting of Al3 + ion with sensitivity of 0.19 mM [99]. Moreover, the dye shows moderately cytotoxicity and can be employed for the detection of intracellular concentration of Al^{3+} ions in living cells. The energy gap between HOMO and LUMO in the probe **50** and **50**–Al^{3+} complexes are 2.6691 eV and 2.1089 eV respectively (Fig. 12). Xu Zheng et al. synthesized a bis(pyridine-2-ylmethyl)amine derivative **51** displays significant colorimetric and fluorescent changes upon binding of Cu^{2+} [100]. **51** has potential candidate for the Cu^{2+} sensing in aqueous solution and mammalian cells. Qi Huang et al. developed a ''off–on'' fluorescent sensor for the detection of Al^{3+} with a high sensitivity and detection limits of 0.23 and 1.90 lM [101]. The sensor **52** was used for the effective sensing of Al(III) furthermore it can be used as a bioimaging reagent for imaging of Al^{3+} in living cells.

A dicyanoisophorone-based turn-on chemodosimeter **53** has been synthesized to detect Cu^{2+} with significant color change [102]. The LOD of chemodosimeter **53** was calculated as low as 0.2 μM for Cu^{2+}. The probe **53** was also successfully applied to fluorescence imaging of Cu^{2+} in HeLa cells. Enze Wang et al. synthesized **54** by condensation of 5-Hydroxymethylfurfural and rhodamine B hydrazide which indicate high selective and reversible colorimetric chemosensor for Cu^{2+} [103]. The high absorbance at 565 nm, molecular fraction close to 0.33, which exhibit the 1:2 complexation (Fig. 13).

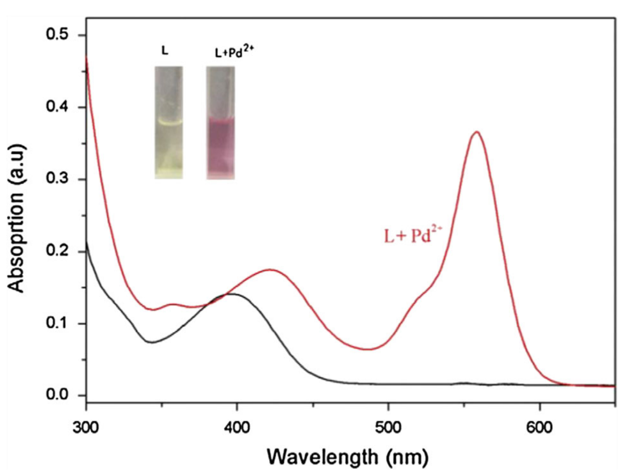

Fig. 10 UV–vis changes of **45** (10 lM) with 5 equiv. of Pd2 + in CH3CN–H2O. 'Reprinted from reference number 95 with permission of Elsevier publication'

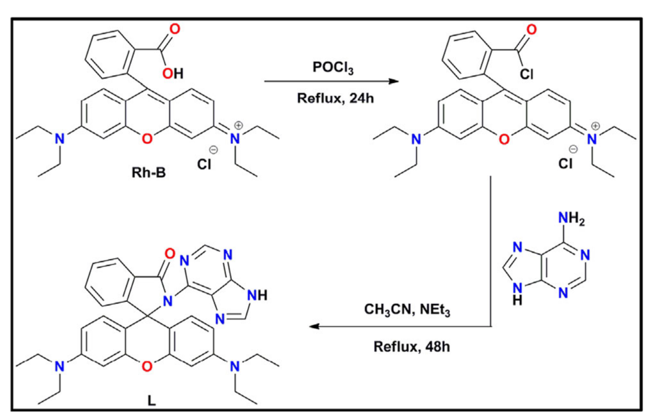

Fig. 11 Chemical structure of Al^{3+} ion selective receptor **50**

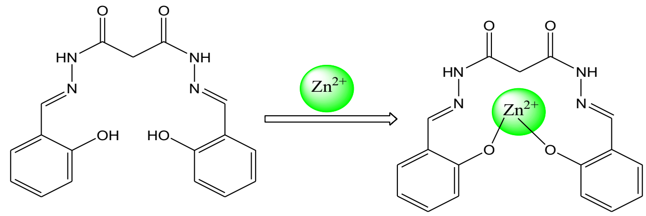

30 30.Zn Complex

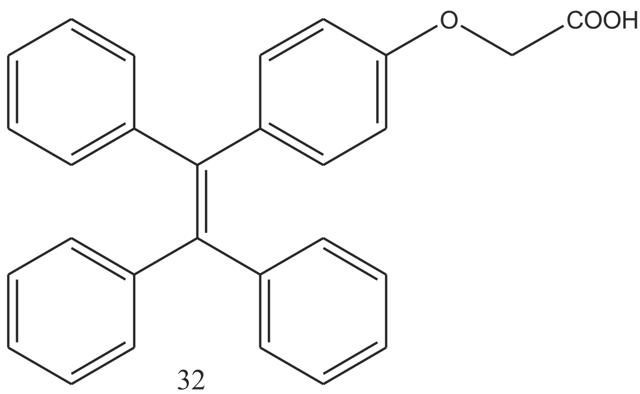

32

Jing-Can Qin et al. synthesized **55a** and **55b** fluorescent probes for Al^{3+}, upon addition of Al^{3+}, they exhibit a large fluorescence enhancement by PET process [104]. More importantly, the lowest detection limits of the sensors for Al^{3+} were determined as 4×10^{-8}M and 8×10^{-8}M (Fig. 14). Vinod Kumar Gupta et al. synthesized probes **56a** and **56b** which displayed excellent "off-on" fluoregenic selectivity with Zn(II) [105]. The results revealed that the sensors provided colorimetric and fluoregenic sensing excellent response with low limit of detection, under neutral conditions. Hak-Soo Kim et al. designed **57** which displayed "OFF–ON–OFF" dual responce for the sensing of Cu^{2+} and Al^{3+} [106]. LOD of the **57** for Cu^{2+} and Al^{3+} were 4.726×10^{-7} and 4.43×10^{-7}M, respectively. The 1:1 complexation was anticipated between **57**and Cu^{2+}/Al^{3+} by the ^{1}H NMR binding studies.

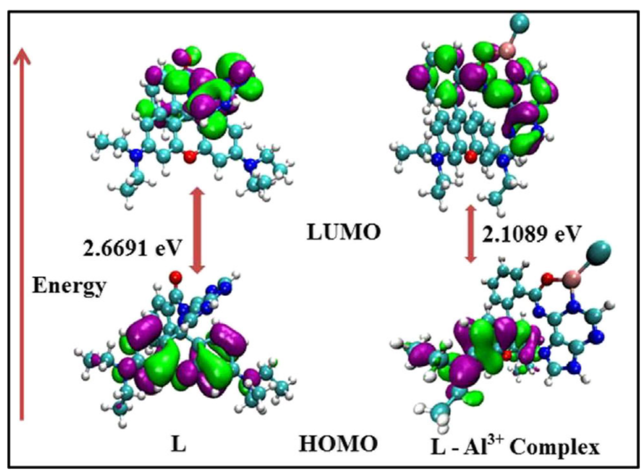

Fig. 12 π-MO's distribution and energy gap between HOMO and LUMO of **50** and **50**–Al3 + complex. 'Reprinted from reference number 99 with permission of Elsevier publication'

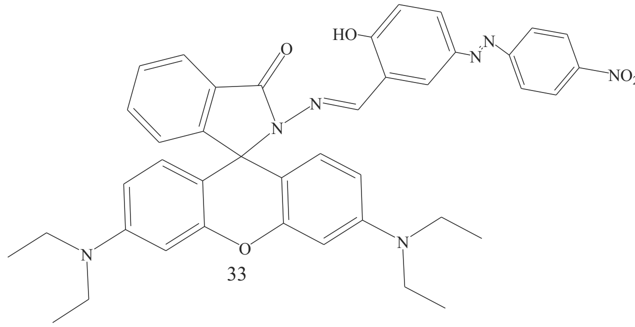

33

Kandasamy Ponnuvel et al. designed chemosensor **58** which shows extremely good sensing ability towards Zn^{2+} ions (Fig. 15) [107]. 1:1 complexation formation is supported by Job's plot and its can be employed for fluorescent imaging of Zn^{2+} (Fig. 16). Jiao Geng et al. developed 4,4,-n-butyl-5,5-(pyridin-4-yl)-2,2,-bithiazol (**59**) and it exhibits high senstivity toward Fe^{3+} with LOD at 0.6 μM. The K_a of [Fe**59**2] is determined at $2.76 \times 10^{3} M^{-2}$[108]. The living cell and zebrafish imaging experiments demonstrated its applicability in biological systems. Fluorenyl-diformyl phenol Schiff (**60**) base shows maximum intensity upon addition of Al^{3+} at 600 nm and the LOD is 6.22×10^{-9}M. [109]. Applicability for DSSC device fabrication of probe shows photovoltaic efficiency 0.021%. Probe N,N–bis((2–hydroxynaphthalen–1–yl)methylene)malonohydrazide (**61**), exhibited selective detection of Al^{3+} ions with a binding constant K_B=5.74 × $10^{9} M^{-1}$ and detection limit 5.78×10^{-8}M [110]. The (**61**2Al^{3+}) complex mechanism was studied by DFT and cell-imaging study shows that the aluminium ion in cells can be detected by **61**.

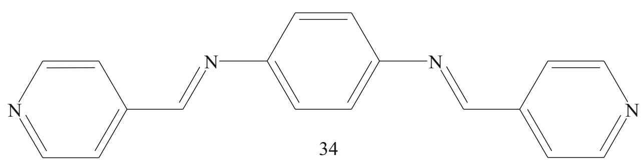

34

Chemosensor **62** displayed 16-time increases in fluorescence for selective detection of Mg^{2+} with limit of detections for Mg^{2+} at 10^{-8}M in DMSO:H_2O (1:5v/v) medium [111]. Sensor **62** has ability to detect Mg^{2+} in cells (Fig. 17). The thioethers **63a** and **63b** have shown excellent selective recognition toward Hg^{2+} with detection limit 6.93×10^{-7}M and 4.79×10^{-7}M respectively [112]. Moreover, ferrocenyl-based sulphone **63c** and **63d** which exhibited more selective recognition toward

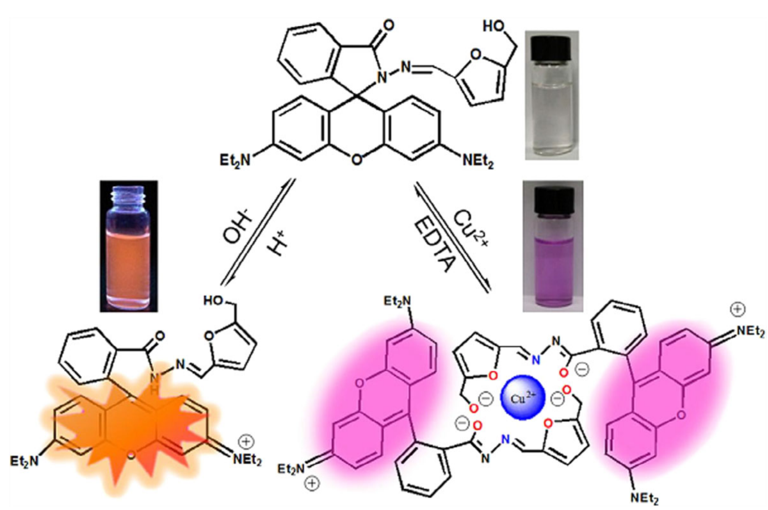

Fig. 13 Proposed mechanism of **54** for H + and Cu2 + respectively. 'Reprinted from reference number 103 with permission of Elsevier publication'

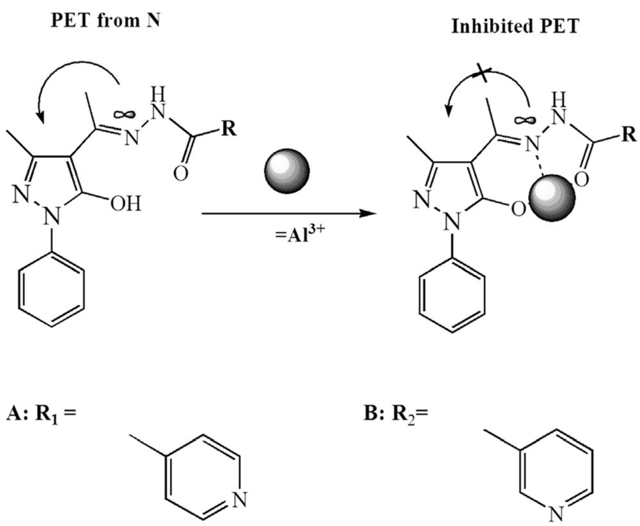

Fig. 14 Proposed mechanisms for detection of Al3 + by receptor **55a** and **55b**. 'Reprinted from reference number 104 with permission of Elsevier publication'

Cu^{2+} and the detection limit values can reach 5.22×10^{-7}M and 4.97×10^{-7}M (Fig. 18). A pyridylvinyl-rhodamine-naphthalimide fluorescent probe **64**, was synthesized which shows recognition ability towards Fe^{3+} and Hg^{2+} [113]. The **64** represented dual-channel behavior, with detection limit at 2.72×10^{-8}M and 9.08×10^{-8}M, and the K_d were calculated to be $4.95 \times 10^{-7}M^{3/2}$ and $6.68 \times 10^{-8}M^{3/2}$, respectively. The probe **65** only showed an enhancement and quenching (naked-eye colour change) in fluorescence for Hg^{2+} and Cu^{2+} respectively [114]. Additionally, the probe was effectively used in cell imaging, indicating its promising application in living cells. A rhodamine derivative (**66**) designed for the detection of Cd^{2+} with LOD of 1.025×10^{-8}M [115]. New emmision peak produce at 590 nm due to recognition of Cd^{2+} ions with **66** in a 1:1 cmplexation with a K_b of $4.2524 \times 10^4 M^{-1}$. **66** has exhibited extremely superior results in Cells imaging.

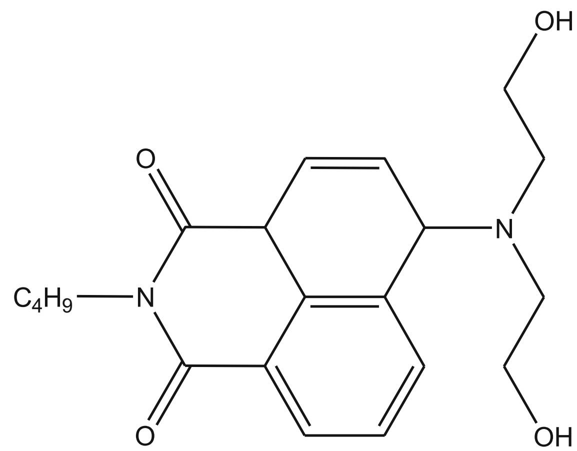

35

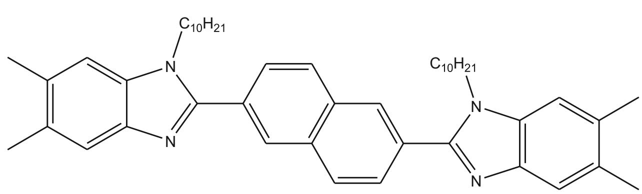

36

A Schiff-base **67** was synthesized and used for detection of Zn^{2+} with on the CHEF and PET mechanisms [116]. The UV–vis spectra of the Zn^{2+} complex exhibit four clear isosbestic points which may be assigned to the ONON moieties binding to Zn^{2+} and complex crystal characterized by X-ray crystallography (Fig. 19). Ujjal Ghosh et al. synthesized meta-di-4-methylpyridyl benzene **68** probe for Hg^{2+} detection [117]. The probe shows a dual fluorescence emission at long wavelength region (350, 425 nm) and theoretical calculation and NMR titration suggest that the probe binds Hg^{2+} through the coordination with two pyridyl nitrogens. A schiff base (**69**) based on 4,5-diazafluorene used for selective sensing of Al^{3+} ions and it shows 1312-time fluorescence enhancement when the Al^{3+} added in the **69** [118]. The LOD found to be at 3.7×10^{-8}M. A sensor (**70**) designed for the effective detection of Cu^{2+} through the PET mechanism [119]. The sensor showed "off–on" fluorescence response with a 120-fold increase toward

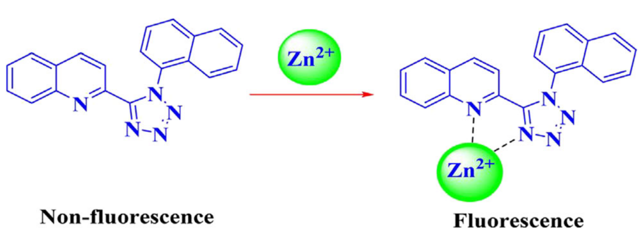

Fig. 15 Proposed mechanism of **58** with Zn^{2+}. 'Reprinted from reference number 107 with permission of Elsevier publication'

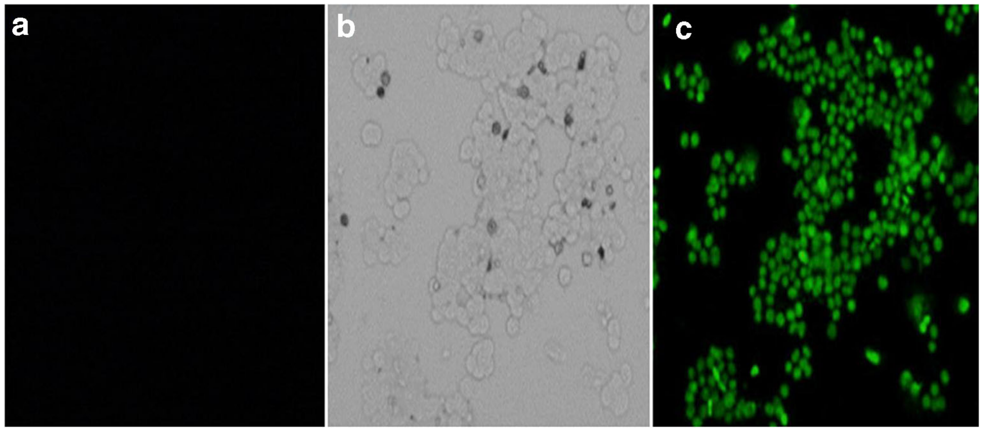

Fig. 16 **a** Image of cells with QT-1, **b** bright-field image of **58** treated MCF7 cells, **c** Image of MCF7 cells with **58** and $ZnCl_2$ (λ_{em} = 460 nm). 'Reprinted from reference number 107 with permission of Elsevier publication'

Cu^{2+}, and its limits of detection were 0.26 mM and 0.17 mM for UV-vis and fluorescence measurements, respectively.

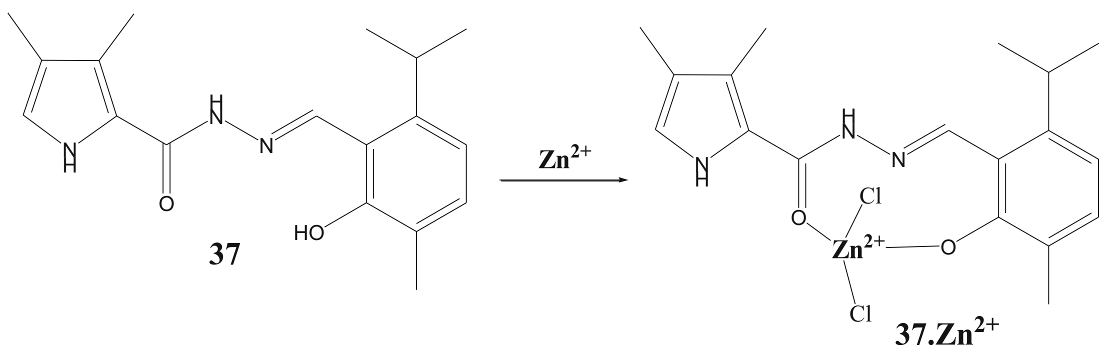

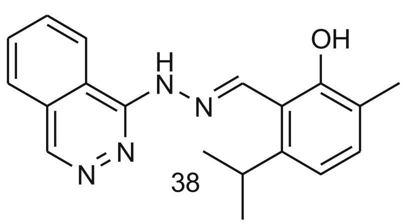

Chemosensors (**71**) which shows excellent sensitivity for Hg(II) with LOD at 1.06μmolL^{-1} [120]. 1:1 complexation is confirmed by ^{1}H-NMR titration (Fig. 20) and interference study (Figs. 21) shows that the good capability of chemosensor for detction of Hg^{2+} in presence of other ions. Rui Yan et al. fabricated a biomimetic chemosensor, **72** used for the detection of zinc(II) and cell imaging [121]. Moreover, cytotoxicity and bioimaging tests were conducted to study the potential bioapplication of the chemosensor. Xianjiao Meng et al.

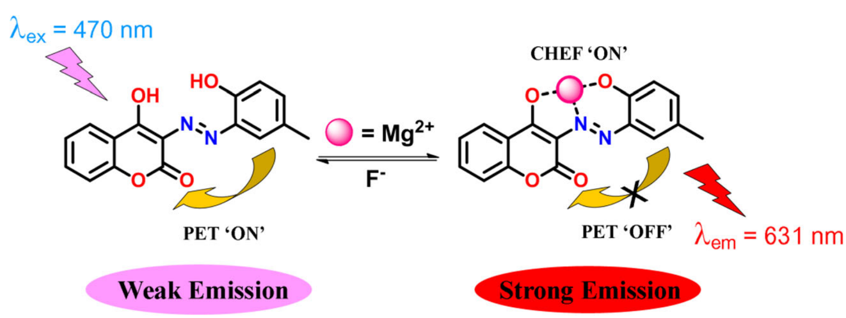

Fig. 17 PET mechanism of **62** with Mg^{2+} ions. 'Reprinted from reference number 111 with permission of Elsevier publication'

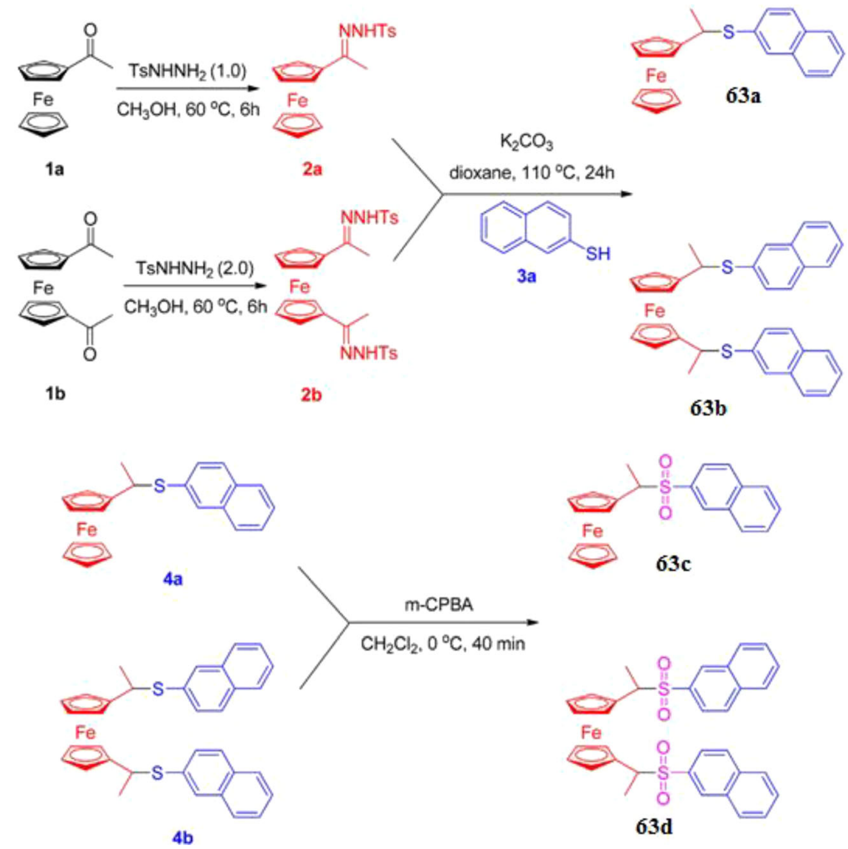

Fig. 18 Chemical structure and synthesis of receptors **63a** to **63d**. 'Reprinted from reference number 112 with permission of Elsevier publication'

synthesized chemosensor, ethyl(E)-2-((2-((2-(7-(diethylamino)- 2-oxo-2H-chromene-3-carbonyl)hydrazono)methyl)quinolin-8-yl)oxy)acetate (**73**), which showed an "on–off" fluorescence response to Pb^{2+} with a 1:1 complexation and LOD determined to be 0.5μmM [122].

A "off-on-off" probe (**74**) displayed the selective detection towards Hg^{2+} with K_a estimated to be 4.66×10^6 and LOD calculated as 2.64×10^{-8}M [123]. Furthermore, the HOMO-LUMO energy gaps of the complex are lower than the free probe (Figs. 22 and 23).

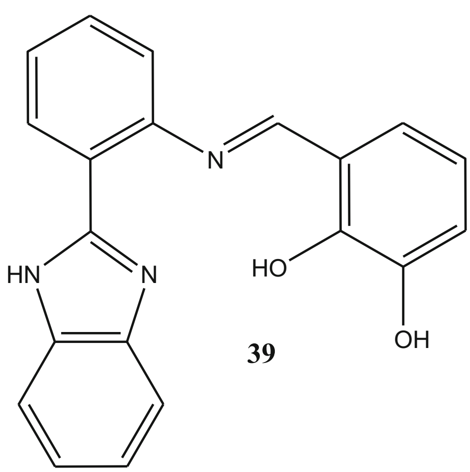

39

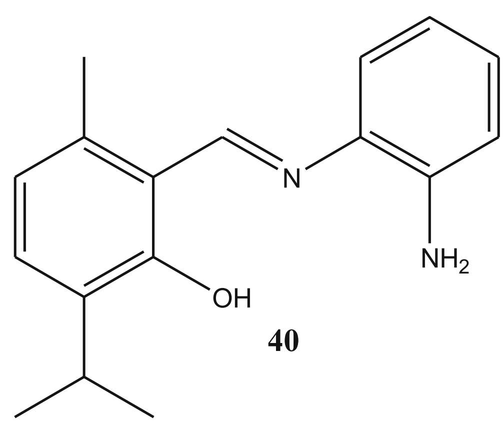

40

Somnath Khanra et al. synthesized imine and azine derivatives **75a, 75b, 75c** and **75d**, shows fluorescence turns ON for Zn^{2+} detection at nano-molar level. The LOD of **75a, 75b, 75c** and **75d** for Zn^{2+} are 32.66 nM, 36.16 nM, 15.20 nM and 33.50 nM respectively [124]. Pravat Ghorai et al. represented economic probe (**76**) for efficient detection of both Zn(II) and

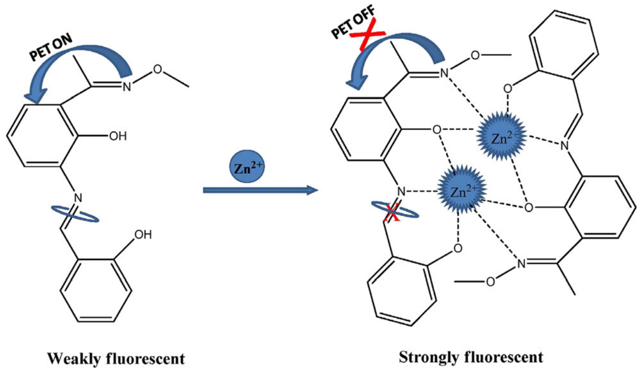

Fig. 19 Chemical structure of sensor **67** and the proposed receptor-metal chelation mechanism. Two metal ions and two ligand molecules are used to express 1:1 stoichiometry of complexation for clarity purpose. 'Reprinted from reference number 116 with permission of Elsevier publication'

Cu (II) with the formation 1:1 complexation confirmed by Job's Plot. The LOD values of both the ions are 2.29×10^{-9}M and 3.67×10^{-9}M, respectively. The probe used for Candida albicans cell fluorescence imaging [125]. Yingying Zhang et al. reported water-soluble probe **77** for the detection of Hg^{2+} in real water samples and showing changed from pale yellow to pink. Probe was confirmed to have low cytotoxicity and excellent cell membrane permeability [126]. Serkan Erdemir et al. developed Triphenylamine appended rhodamine (**78**) (Fig. 24) was built as a selective fluorescent probe for Al^{3+} and Hg^{2+} ions with 1:1 complexation confirmed by by job plot analysis. The LOD of 78 for sensing Al^{3+} and Hg^{2+} are down to 71.8 nM and 0.48 μM, respectively [127].

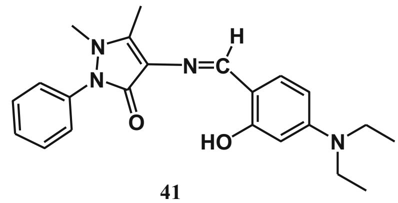

41

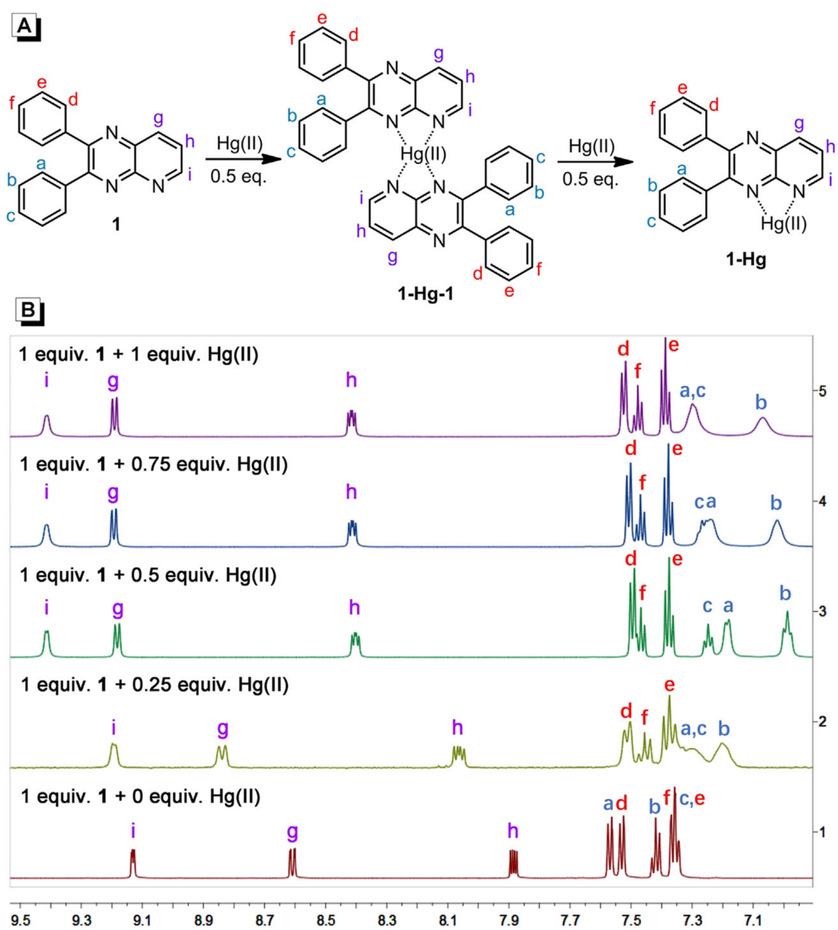

Fig. 20 **A** Mechanism for **71** and 71.Hg^{2+}. **B** ^{1}H-NMR of **71** in the presence of different cncentration of Hg^{2+}. 'Reprinted from reference number 120 with permission of Elsevier publication'

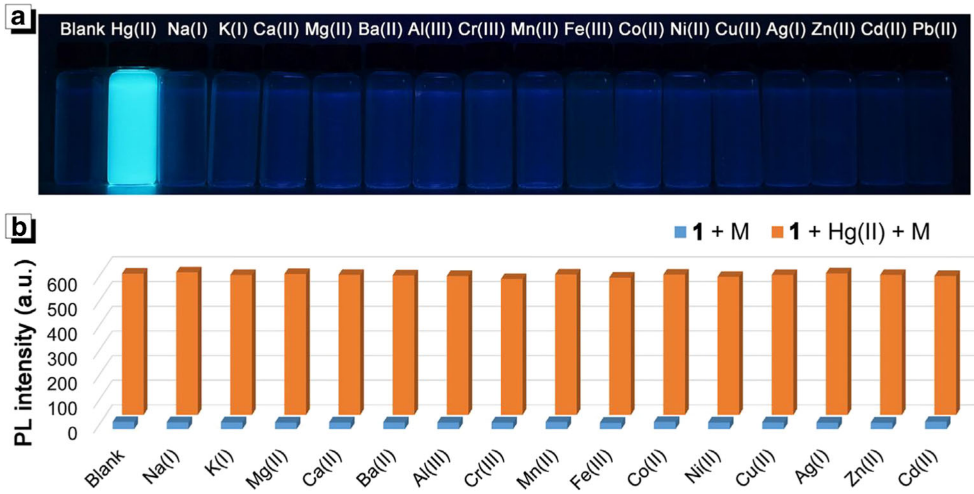

Fig. 21 **A** Image of **71** and with the additin of metals under irradiation of 365 nm UV light. **B** Interference study. 'Reprinted from reference number 120 with permission of Elsevier publication'

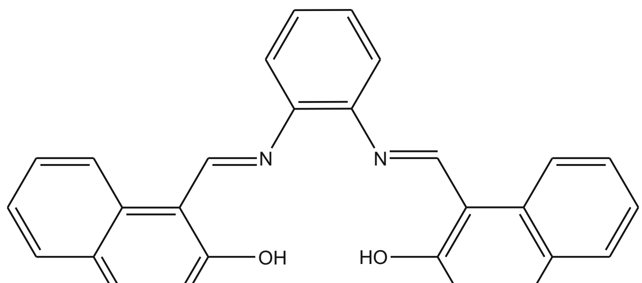

42

Kalyani Rout et al. fabricated a triazole-based probe (**79**) which have good sensing ability for Cu^{2+} and Pb^{2+} ions with the naked eye colour change. The **79** shows its potential application in real samples, living cells and building of molecular logic gate [128]. Yunfan Yang et al. developed fluorescence probe **80** for detecting Hg^{2+} and OCl^{-} ions. The FMO and overlap between hole and electron analyses confirmed that the interaction between **80** and Hg^{2+} impeded the ESICT behavior [129]. Vishaka V. H et al. demonstrated a biocompatible fluorescent receptor (**81**) for detection of Fe^{3+} upto 8.2 nM LOD. Receptor imaging Fe^{3+} in cells is a significant increase towards biosensing and cytotoxicity studies also proved the nontoxic nature of this receptor [130]. Jae Min Jung et al. synthesized naphthol-based chemosensor **82** for the Zn^{2+} sensing through $\pi \rightarrow \pi^*$ transition with a unique fluorescence enhancement (Fig. 25**)**. We confirmed the sensing properties of **82** toward CN − and Zn^{2+} with theoretical calculation [131].

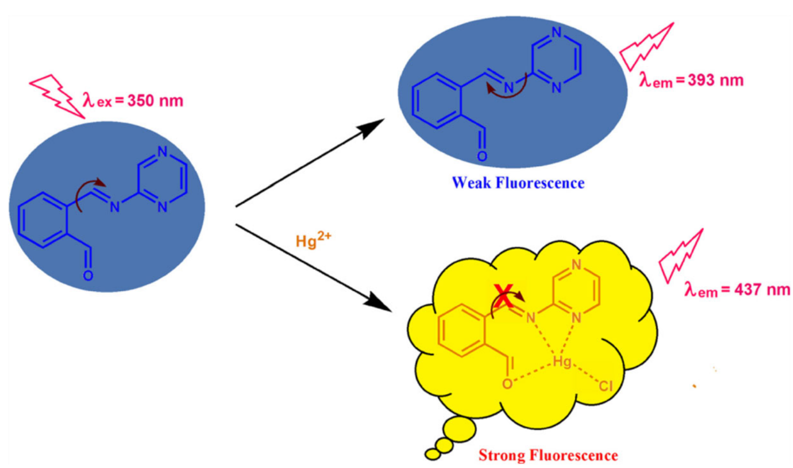

Fig. 22 Proposed sensing mechanism of **74** with Hg^{2+} ion. 'Reprinted from reference number 123 with permission of Elsevier publication'

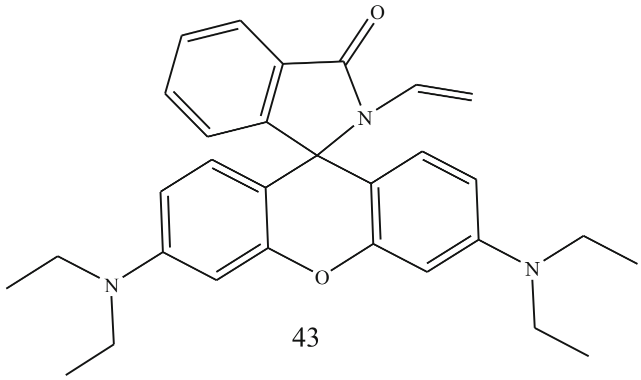

43

Yaping Zhang et al. synthesized a fluorescent receptor **83** by attaching a diarylethene molecule to a functional group for the detection of Al^{3+} and Zn^{2+} at detection limit is very low. Moreover, based on the properties of **83**, we designed a logic circuit, and that also can be used for water sample testing [132]. Jeya Shree Ganesan et al. synthesized pyrazole bearing imidazole derivative **84** for the selective detection of Al3+/Fe3 + ions with 1:1 binding stoichiometry confirmed by Job's plot. The LOD of **84** with Al3+/Fe3 + was calculated as 2.12×10^{-7}M and 1.73×10^{-6}M, respectively [133]. Pinkesh G. Sutariya et al. reported calix[4]arene conjugate bearing 1-aminoanthraquinone with amide linkage (**85**) recognize three metals La^{3+}, Cu^{2+} and Br^{-} with detection limit 0.88 nM for La^{3+}, 0.19 nM for Cu^{2+} and 0.15 nM for Br^{-} (Fig. 26**)** [134]. Akshay Krishna T G et al. developed isatin appended Schiff's base probes (**86a-86c**) and characterized by spectroscopic techniques. The sensing ability of probe towards Hg^{2+} ions was established through UV-Visible techniques and achieved detection limit at ppm levels [135].

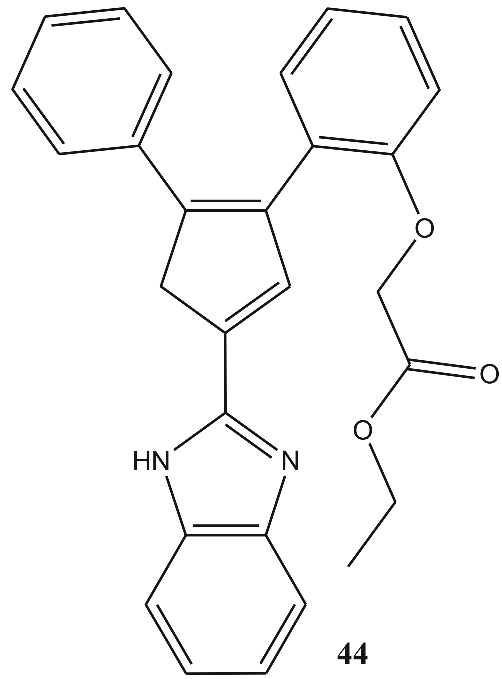

44

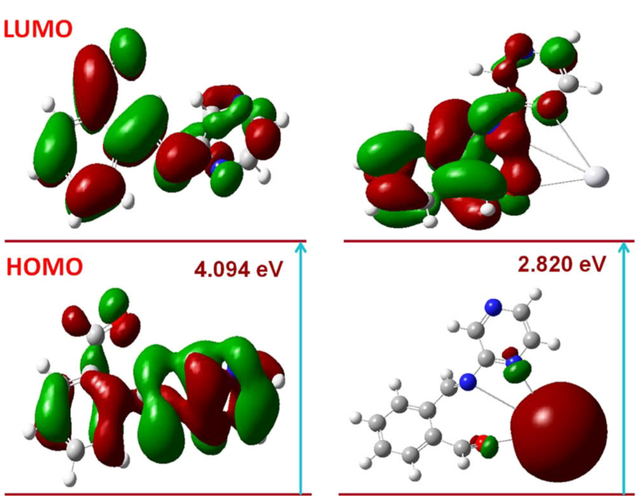

Fig. 23 Optimized structural geometry of probe and its complexes (**74** and **74**-Hg^{2+} from left to right). 'Reprinted from reference number 123 with permission of Elsevier publication'

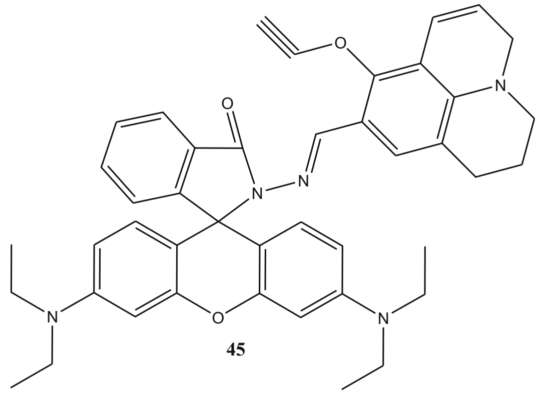

45

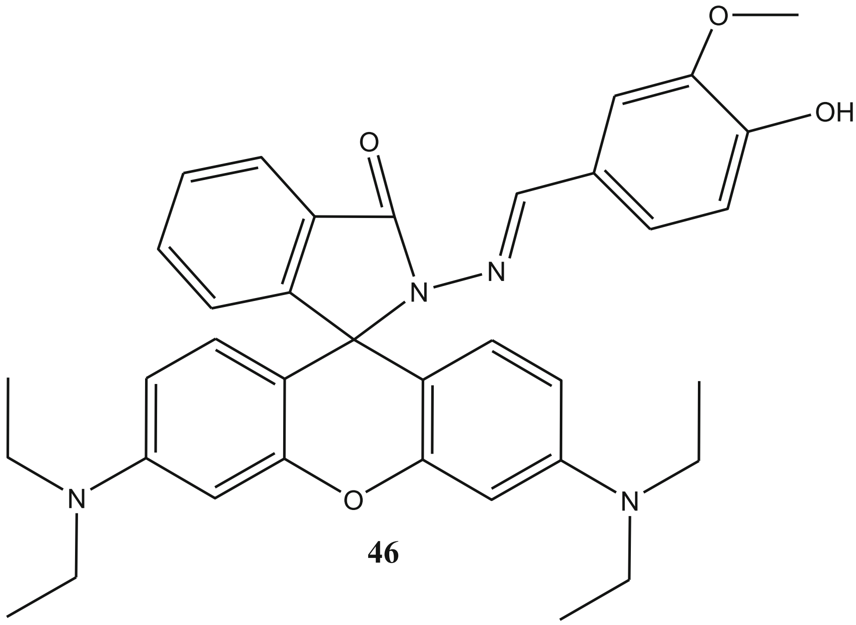

46

Suman Srivastava et al. synthesized a fluorescent probe **87** for the selective sensing for Fe^{3+} and Hg^{2+}. "The LOD of **87** toward Fe^{3+} and Hg^{2+} has been found at 4.0 ppb and 1.0 ppb, respectively and also shows fluorescence signalling both in vitro and in vivo" [136]. Awad I. Said et al. developed rhodamine-pyrazole based probe **88** which has ability to detect the Cu^{2+}, Fe^{3+}, Al^{3+}, Hg^{2+} and Ni^{2+} discriminately. Furthermore, the probe exhibited a high potential for logical operations and INHIBIT logic gates [137]. Jessica C. Berrones-Reyes et al. developed (S,E)-11-amino-8-((8-hydroxybenzylidene)amino)-11-oxopentanoic acid (**89**) receptor for the Zn^{2+} ions detection with LOD of 1.20 mM [138]. Barbara Panunzi et al. reported a complex of pyridyl/phenolic/benzothiazole functionalized ligand (**90**) with $Zn(CH_3COO)$. The structural and photoluminescence properties of the complex were investigated by X-ray diffraction and DFT study and LOD at 375 nM (Fig. 27) [139].

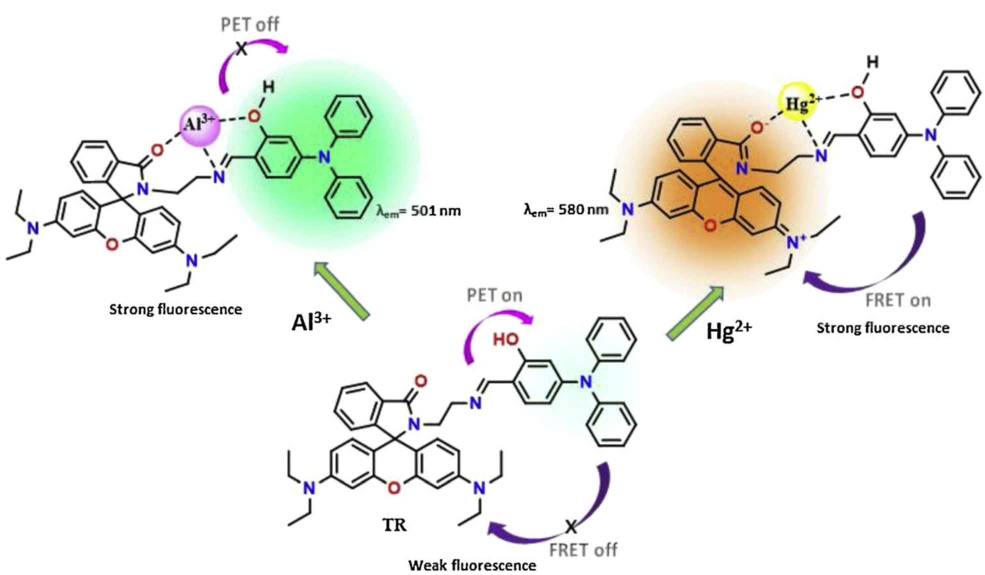

Fig. 24 Proposed mechanism for Al^{3+} and Hg^{2+} detection by probe **78**. (Reprinted from reference number 127 with permission of Elsevier publication)

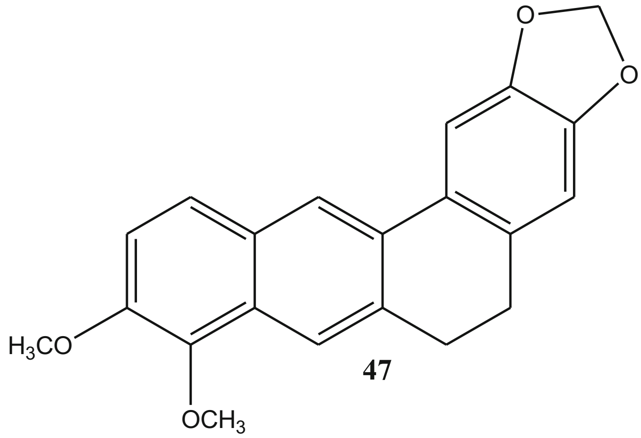

47

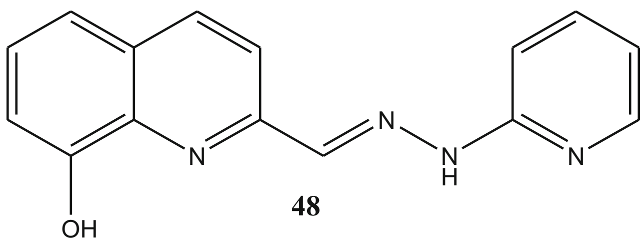

48

Shengling Li et al. reported highly selective probe **91** for the recognition of Cu^{2+} and HSO_3^- with detection limit of the sensor **91** was 0.36 mM to Cu^{2+} and 1.4 mM to HSO_3^- (Fig. 28**)** [140]. Yun-Qiong Gu et al. developed sensor **92**, based on pyrazolopyrimidine for the simultaneous detection of Ni^{2+} and Cu^{2+} ions with LOD at 8.9 nM for Ni^{2+} and 8.7 nM for Cu^{2+} and fluorescence imaging in T-24 cells was investigated because of the low cytotoxicity of **92** [141]. Jianwei Xu et al. synthesized Ferrocene–based naphthalene receptors **93a** and **93b** and behaved as naked-eye receptor for Cu^{2+} and with low detection limit. Furthermore, **93a** and **93b** were nontoxicity and receptor **93a** exhibited certain antibacterial activity (Fig. 29**)** [142]. Qiang Zhang et al. fabricated multi-response probe **94** for the detecting Al^{3+}, Cu^{2+} and Mg^{2+} in ethanol. The optimized structure of the sensor 94 and its sensing mechanism for Al^{3+}, Cu^{2+} and Mg^{2+} were confirmed by the calculations of TD-DFT methods Fig. 30 [143].

Fig. 25 Sensing mechanism of Zn^{2+} by **82**. (Reprinted from reference number 131 with permission of Elsevier publication)

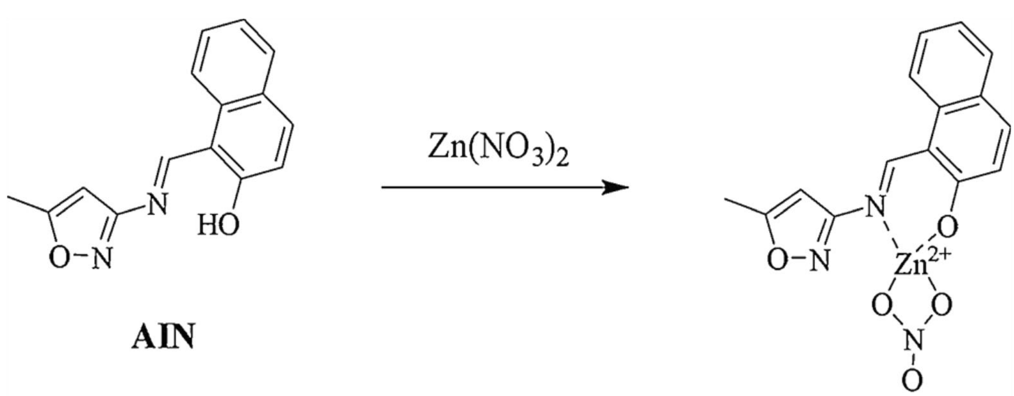

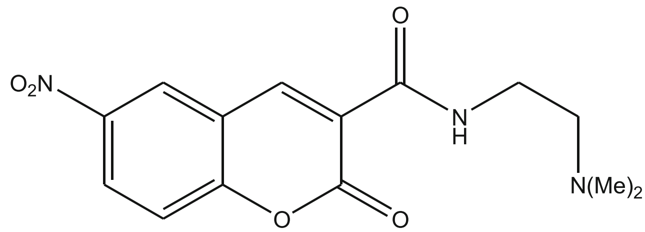

49

Xiaowei Mao et al. reported 1,2-bis-(2-pyren-1-ylmethylamino-ethoxy)ethane (**95**) brought to the surface of GNs via $\pi-\pi$ stacking, which shows Mn^{2+} sensing with 641 LOD of 4.6×10^{-5}M (Fig. 31). These sensing capabilities of **95** in living cell make it applicable in intracellular tracking, intracellular imaging, etc. [144]. Jianping Guan et al. developed a luminophor, **96**, which showed a sensitive fluorescence response to Fe^{2+} with low detection limits of 115.2 nM. Sensing mechanism indicates that fluorescence-quenched due to Fe^{2+} chelate with the oxygen and nitrogen of **96** (Figs. 32) [145]. Gyeong Jin Park et al. synthesized a colorimetric probe **97** for Co^{2+} detection with changing its color from yellow to orange. Furthermore **97** could be used as a practical, visible colorimetric test kit for Co^{2+} [146]. R. P. Cox et al. developed Crown ethers (**98a and 98b**) for sensing of cations, via changes in absorption/emission and with a 1:1 addition of Na^+ or K^+, providing clear colourimetric readout [147].

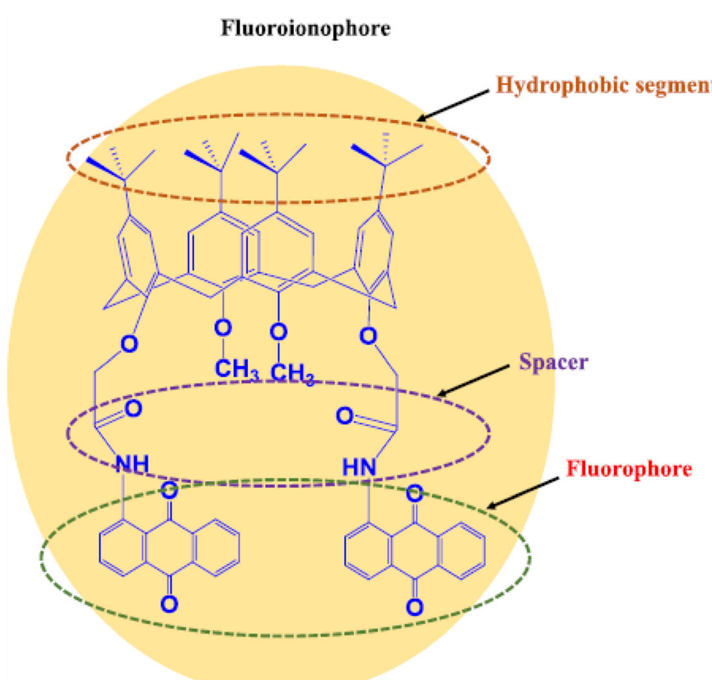

Fig. 26 Structure of Probe 85. (Reprinted from reference number 134 with permission of Elsevier publication)

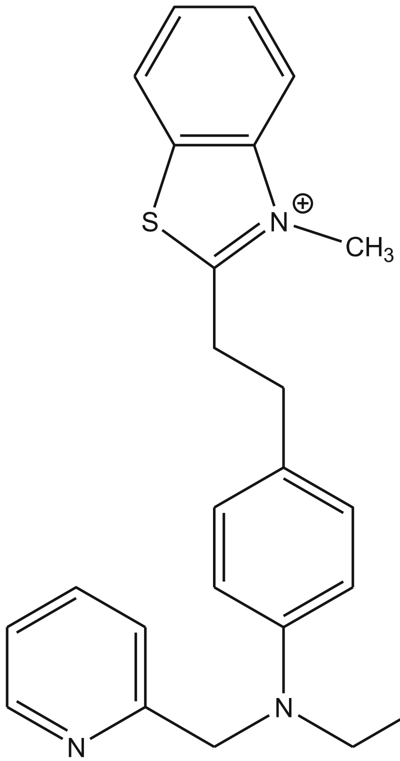

51

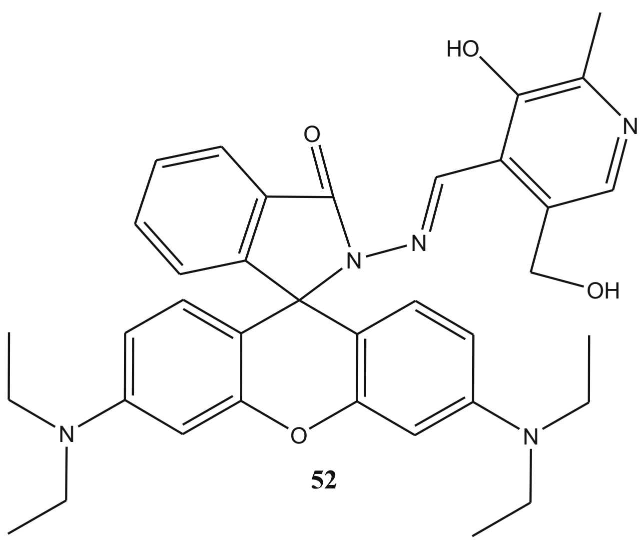

52

Minoo Bagheri et al. developed fluorescent MOF sensor, **99** for the ca.$^{2+}$ sensing concentrations similar to that of blood plasma. The two dimensional signal transduction produce by **99** can reduce interfering responses from the environment and thus generate outstanding sensitivity (Fig. 33) [148]. Jing-Ru Zhou et al. synthesized tripodal amide based probe (**100**), for the colorimetric sensing for cobalt(II) ions by an obvious color change from colorless to yellow [149]. Xiaopeng Yang et al. reported turn on NIR-fluorescent probe **101** based ICT for detection of Fe^{2+} with excellent sensitivity (DL = 4.5 μM) (Fig. 34), rapid response (15 min) and "naked-eye colorimetric sensor" [150]. Diana Pendin et al. synthesized a fluorescent ca^{2+} sensor **102**, shows ratiometric ca^{2+} indicator. **102** binds ca^{2+} with a dissociation constant of &1.5 mm in vitro [151].

Minuk Yang et al. synthesized sensor with pyridyl and carbohydrazide (**103**) gives visibly blue colour in the presence of Fe^{2+} and yellow when exposed to Co^{2+} and Cu^{2+}. The binding constants of the sensor are: Fe^{2+}: 1.0 ×

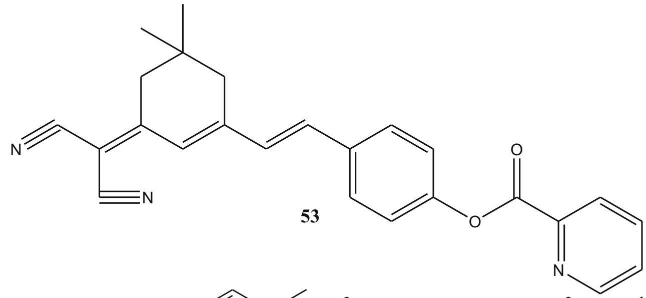

53

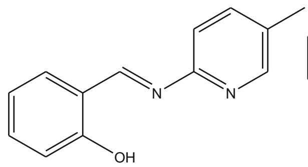

56a

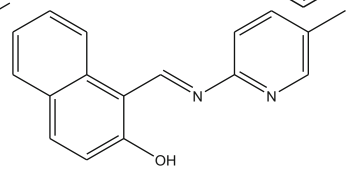

56b

$10^9 M^{-2}$, Co^{2+}: $2 \times 10^9 M^{-2}$, and Cu^{2+}: $3.0 \times 10^9 M^{-2}$ [152]. Meng-Xia Huang et al. synthesized fluorescence probe (**104**) showed a outstanding fluorescence enhancement toward Cd^{2+} with a LOD of 29.3 nM. The binding stoichiometry between 10^4 and Cd^{2+} was 2:1 as confirmed by the Job's Plot and ^{1}H NMR titration experiment (Fig. 35**)** [153]. Suman Swami et al. reported sensor (**105a** to **105c**) for excellent selectivity and sensitivity towards detection of Mn^{2+} and Zn^{2+} ions using UV-visible titration, fluorescent titration. Job's plot methods revealed that sensor interact with Mn^{2+} and Zn^{2+} ion in 1:1 and 1:2 binding stoichiometry respectively [154].

Azzurra Sargenti et al. presented fluorescent sensor, **106b** for the quantitative assessment of total intracellular Mg content. The **106b** accurately quantify the intracellular total Mg in much smaller samples than **106a**, also displaying an increased

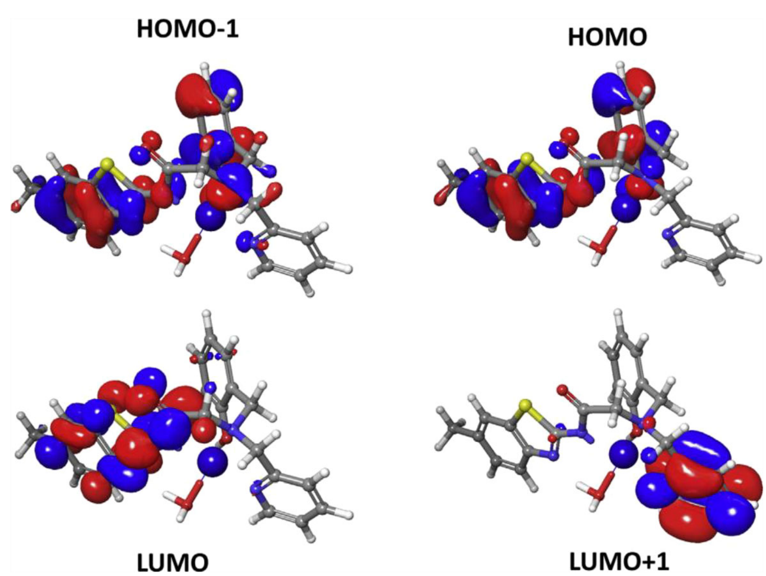

Fig. 27 Frontier orbitals representation of Zn-**90**(H2O). (Reprinted from reference number 139 with permission of Elsevier publication)

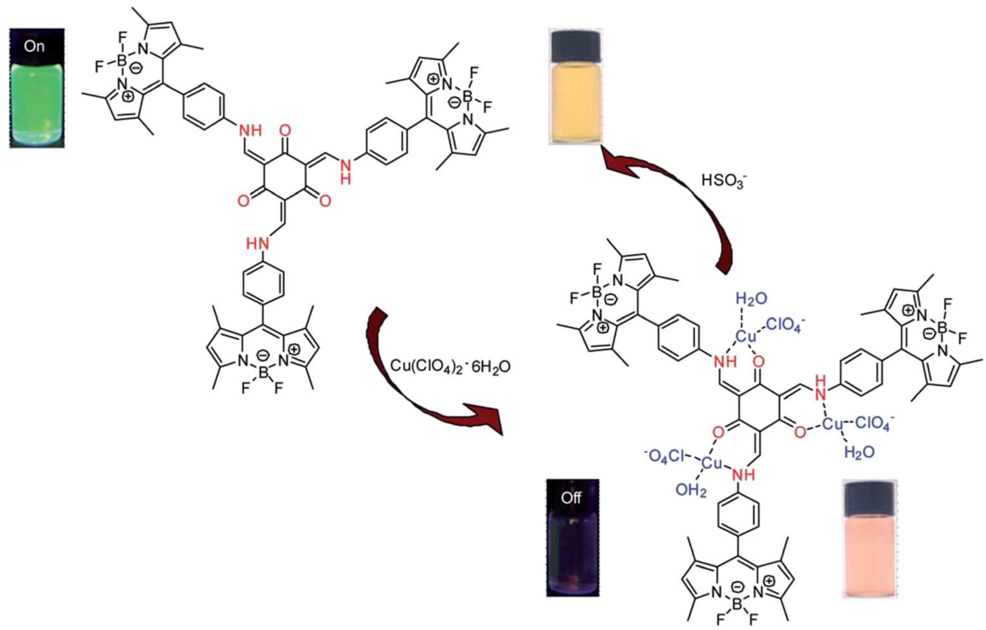

Fig. 28 The possible mechanism of **91**-Cu2 + with HSO3. (Reprinted from reference number 140 with permission of Elsevier publication)

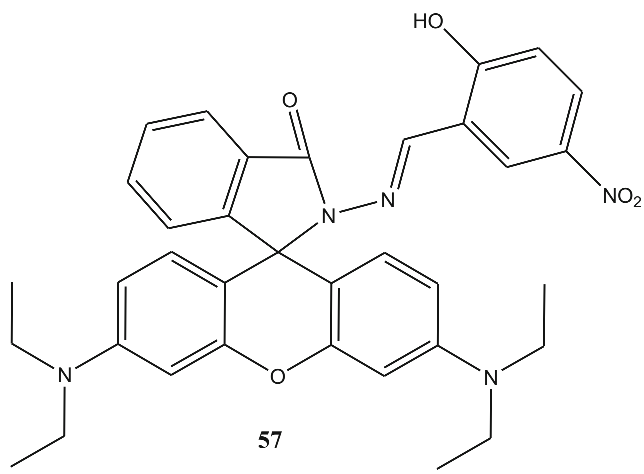

57

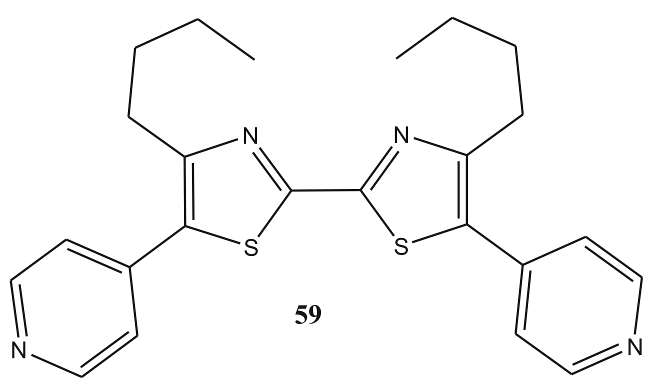

59

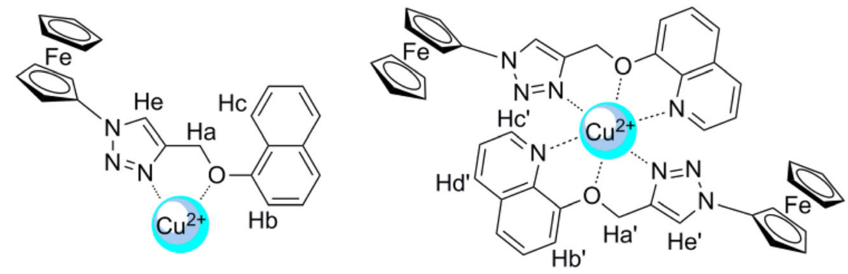

Fig. 29 Proposed binding mode for **93a** and **93b** with Cu2+. (Reprinted from reference number 142 under Creative Commons Attribution-NonCommercial 3.0 Unported Licence of RSC publication)

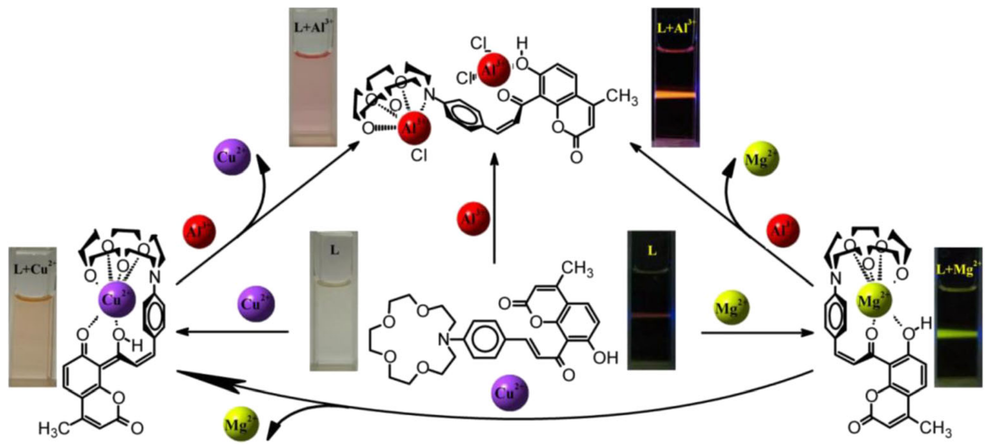

Fig. 30 Proposed binding modes of **94** for Al3+, Cu2 + and Mg2+ .(Reprinted from reference number 143 with permission of Elsevier publication)

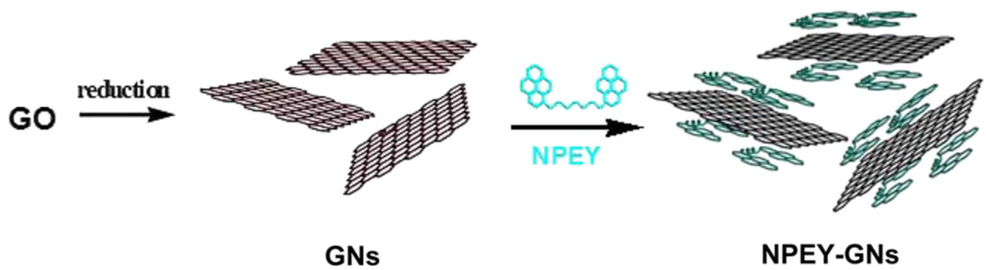

Fig. 31 Synthetic Route for **95.**(Reprinted from reference number 144 with permission of ACS publication)

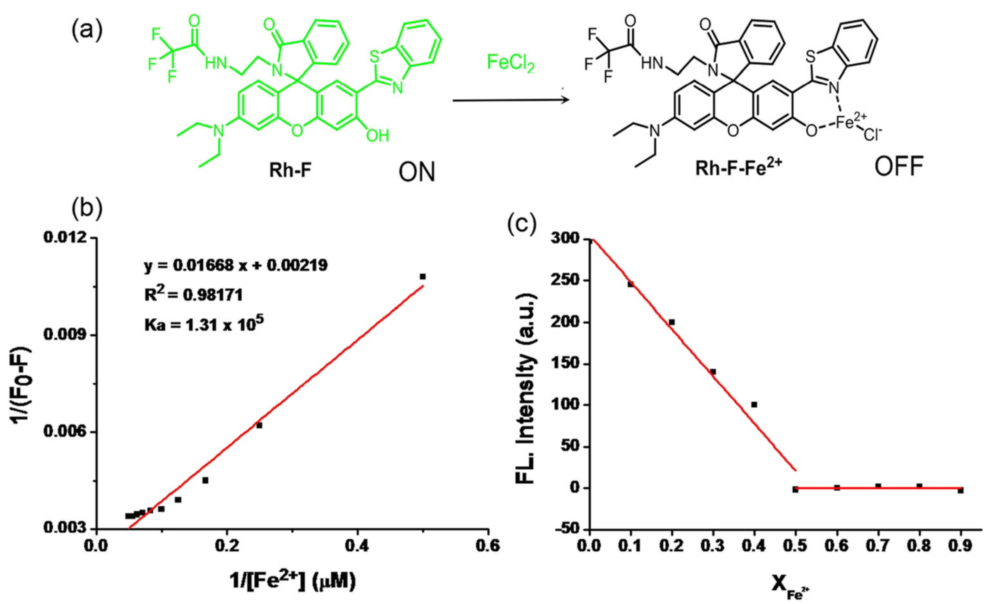

Fig. 32 **a** Sensing mechanism of the **96** probe for Fe^{2+}; **b** Benesi-Hildebrand plot of **96** for Fe^{2+}; **c** Job's plot of **96** with Fe^{2+}. (Reprinted from reference number 145 with permission of Elsevier publication)

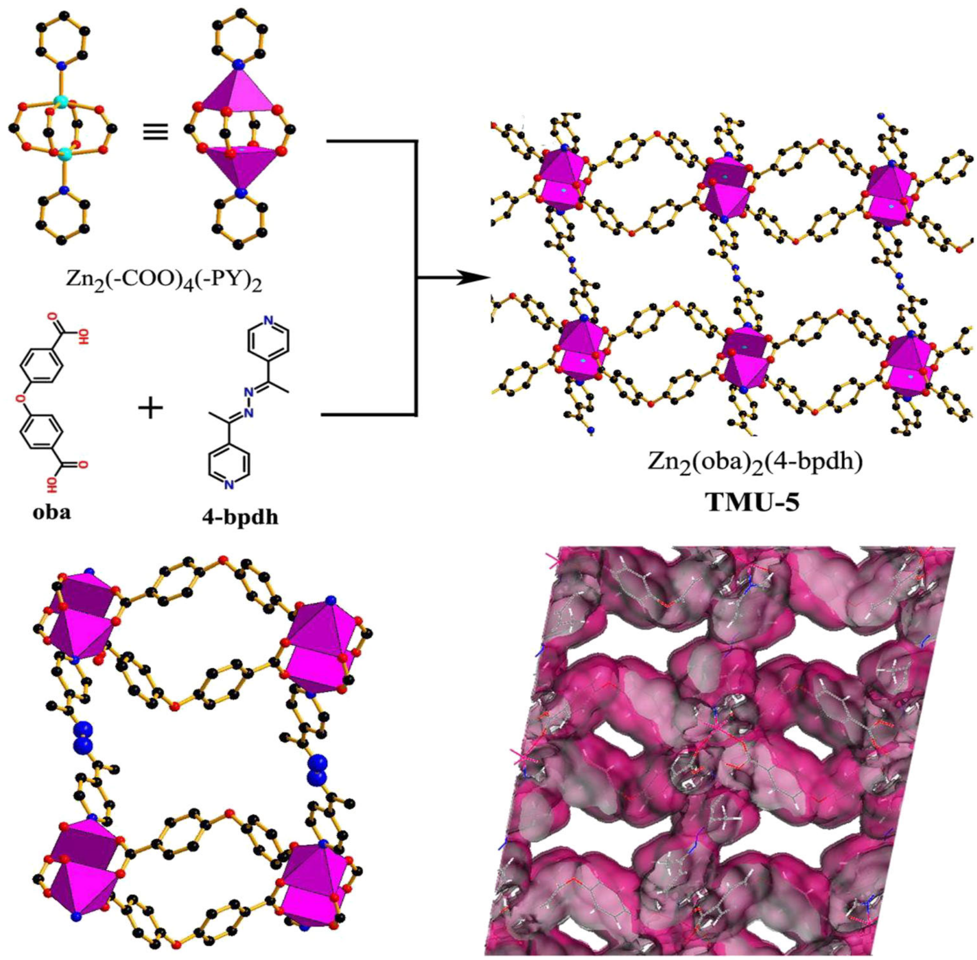

Fig. 33 Structure of **99**. (Reprinted from reference number 148 with permission of ACS publication)

stable intracellular staining [155]. Bing Zhao et al. developed probe containing 1H-phenanthro[9,10-d]imidazole (**107**) moieties linked to double ethylenediamino units for the detection of Ag^+ with LOD calculated at1.01 × 10^7M. The 1:1 binding stoichiometry of L–Ag + complex was confirmed by Job's plot and ESI-MS (Fig. 36) [156]. Juhye Kang et al. reported

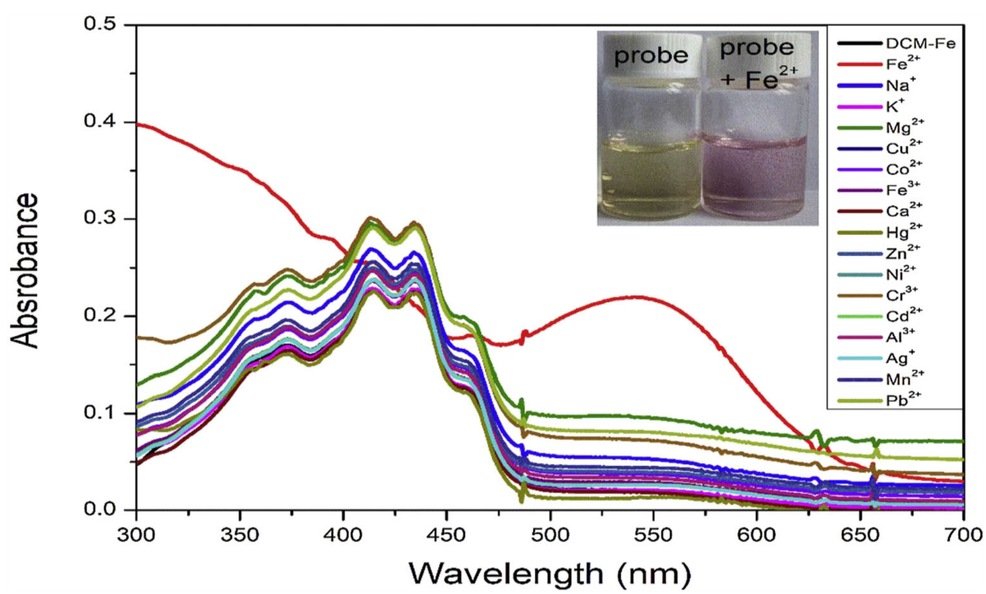

Fig. 34 The UV–vis absorption spectrum of probe **101**-Fe response to Fe^{2+} and other various metal ions. (Reprinted from reference number 150 with permission of Elsevier publication)

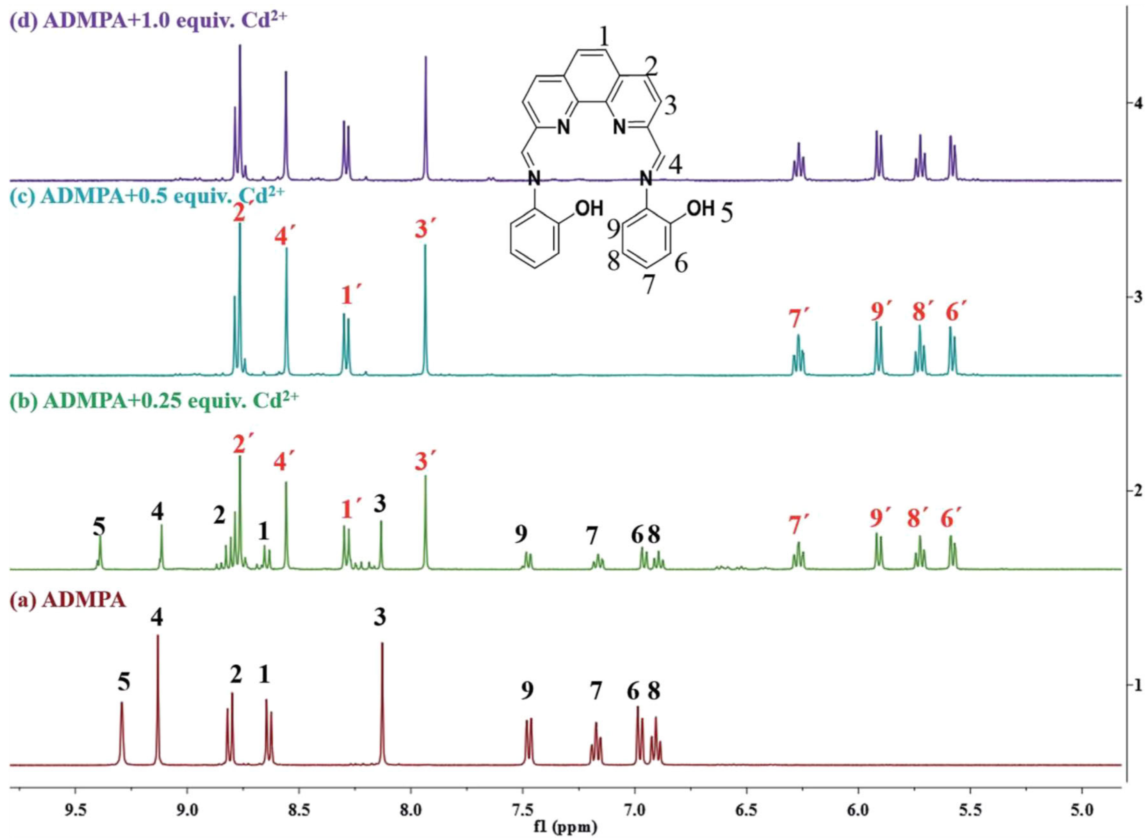

Fig. 35 1H NMR titration of **104** and **104** with Cd2+ (DMSO-d6) for (**a**) **104** only, (**b**) ADMPA with 0.25 equiv. of Cd2+, (**c**) **104** with 0.5 equiv. of Cd2 + and (**d**) **104** with 1.0 equiv. of Cd2+. (Reprinted from reference number 153 with creative common licence 3.0 RSC publication)

sensor of bispicolylamine (**108**) covalently attached to coumarin for the sensing of Mg^{2+}. The formation of a 1:2 complex between the sensor and Mg^{2+} ions was confirmed based on NMR as well as Job's plot [157].

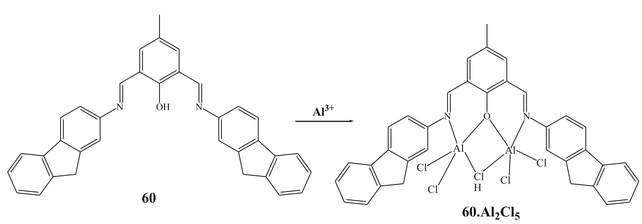

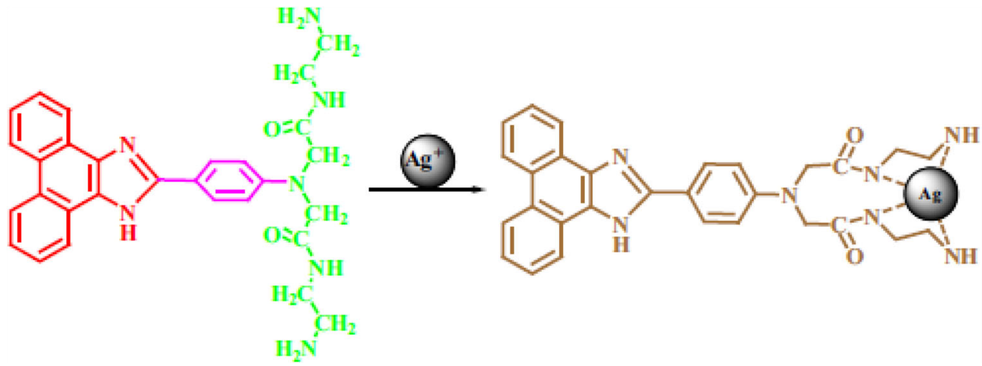

Fig. 36 Possible recognition pattern between compound **107** and Ag^{+}. (Reprinted from reference number 156 with permission of Elsevier publication)

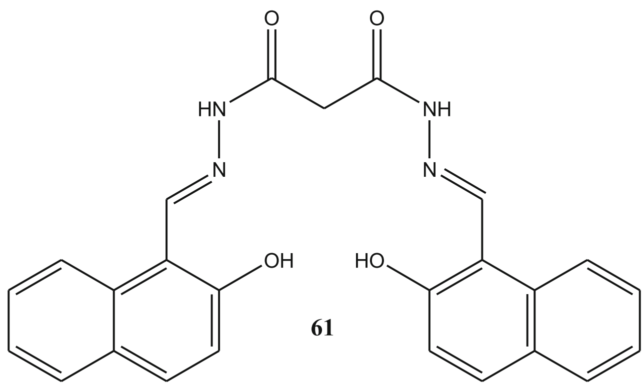

61

Concluding Remarks

The significance and allied adverse consequences of the cationic presence in biological and environmental systems have recognized. Therefore, attention has been given towards the developing of cationic sensors. The sensors were classified into several categories according to their main moiety, such as rhodamine, anthracene, pyrene, imine, quinoline, benzimidazole, BODIPY and nanoparticles based sensing systems. In this review, a huge number of diverse approaches for the development of sensors for cationic ions have been discussed and successfully applied to monitor environmental metal concentrations with high accuracy, precision, reproducibility with a low detection limit is a challenging area from a present day perspective.

References

1. Atood JL, Davies JED, MacNicol DD, Vogetle F (1996) Comprehensive supramolecular chemistry, ed. Elsevier Exeter
2. Valeur B, Leray I (2000) Design principles of fluorescent molecular sensors for cation recognition. Coord Chem Rev 205:3–40
3. Lehn JM (1995) In: Supramolcular chemistry-concept and perspective. VCH, Weinheim
4. Silva AP, Gunaratne HQN, Gunnlaugsson T, Huxley AJM, McCoy CP, Rademacher JT, Rich TE (1997) Signalling recognition event with fluorescent sensors and switches. Coord Chem Rev 97:1515–1566
5. Atwood JL, Holman KT, Steed JW (1996) Chem Commun. 1401–1407
6. Sahoo SK, Sharma D, Bera RK, Crisponi G, Callan JF (2012) Iron(III) selective molecular and supramolecular fluorescent probes. Chem Soc Rev 41:195–7227. https://doi.org/10.1039/c2cs35152h
7. Lehninger AL (1976) Biochemistry. Worth Publishers, New York
8. Lee JD (2008) Concise of Inorganic Chemistry. Wiley, India
9. Zheng YJ, Orbulescu J, Ji XJ, Andreopoulos FM, Pham SM, Leblanc RM (2003) J Am Chem Soc 125:2680–2686
10. Quang DT, Kim JS (2010) Chem Rev 110:6280–6301
11. Zhou Y, Kim HN, Yoon J (2010) Bioorg Med Chem Lett 20:125
12. Kaim W, Schwederski B (1995) Bioinorganic Chemistry
13. Jacobs A (1977) Blood 50:433–439
14. Udhayakumari D, Naha, S, Velmathi S (2016) Colorimetric and Fluorescent chemosensors for Cu2+. A comprehensive review from the year 2013-15, Anal. Methods. https://doi.org/10.1039/C6AY02416E

15. Zhang YM, Qu WJ, Gao GY, Shi BB, Wu GY, Wei TB, Lin Q, Yao H (2014) A highly selective dual-channel chemosensor for mercury ions: utilization of the mechanism of intramolecular charge transfer blocking. New J Chem 38:5075–5080
16. Goswami S, Chakraborty S, Paul S, Halder S, Panjac S, Mukhopadhyay SK (2014) A new pyrene based highly sensitive fluorescence probe for copper(II) and fluoride with living cell application. Org Biomol Chem 12:3037–3044
17. Fegade U, Singh A, Krishna Chaitanya G, Singh N, Attarde S, Kuwar A (2014) Highly selective and sensitive receptor for Fe3+ probing. Spectrochim Acta Part A Mol Biomol Spectrosc 121: 569–574
18. Huang C-B, Li H-R, Luoc Y, Xu L (2014) A naphthalimide-based bifunctional fluorescent probe for the differential detection of Hg2 + and Cu2 + in aqueous solution. Dalton Trans 43:8102–8108
19. Zhou J-R, Lui D-P, He Y, Kong X-J, Zhang Z-M, Ren Y-P, Long L-S, Huang R-B, Zheng L-S (2014) A highly selective colorimetric chemosensor for cobalt(II) ions based on a tripodal amide ligand. Dalton Trans 43:11579–11586
20. Liu J, Wu K, Li S, Song T, Han Y, Li X (2013) A highly sensitive and selective fluorescent chemosensor for Pb2+ ions in an aqueous solution. Dalton Trans 42:3854–3859
21. Chen G, Guo Z, Zeng G, Tang L (2015) Fluorescent and Colorimetric Sensors for Environmental Mercury Detection. Analyst. https://doi.org/10.1039/C5AN00389J
22. Zhou Y, Zhang J, Zhang L, Zhang Q, Ma T, Niu J (2013) Dyes Pigm 97:148
23. Udhayakumari D, Suganya S, Velmathi S (2013) J Lumin 141:48
24. Ping X, Cuicui P, Yingjie Z, Xiangxue K, Juanjuan S, Maoyou X, Zhiqiang S (2012) Tunable fluorescent pH sensor based on water soluble perylenetetracarboxylic acid/Fe3+. Luminescence 27: 307–309
25. Chen X, Hong H, Han R, Zhang D, Ye Y, Zhao YF (2012) A new bis(rhodamine)-based fluorescent chemosensor for Fe3+. J Fluoresc 22:789–794
26. Jung H, Singh N, Jang DO (2008) Highly Fe^{3+} selective ratiometric fluorescent probe based on imine-linked benzimidazole. Tetrahedron Lett 49:2960–2964
27. Saleem M, Lee KH (2015) Optical sensor: a promising strategy for environmental and biomedical monitoring of ionic species. RSC Adv. https://doi.org/10.1039/C5RA11388A
28. Tang L, Dai X, Zhong K, Wen X, Wu D (2014) A phenylbenzothiazole derived fluorescent sensor for Zn(II) recognition in aqueous solution through "Turn-On" excited-state intramolecular proton transfer emission. J Fluoresc 24:1487–1493
29. Sivaraman G, Sathiyaraja V, Chellappa D (2014) Turn-on fluorogenic and chromogenic detection of Fe(III) and its application in living cell imaging. J Lumin 145:480–485
30. Zhao L, Chen X, Guo F, Gou B, Yang C, Xia W (2014) Luminescent properties and logic nature of a crown Schiff base responding to sodium ion and zinc ion. J Lumin 145:486–491
31. Dudina NA, Antina EV, Guseva GB, Vyugin AI (2014) The high sensitive and selective "Off-On" fluorescent Zn2+ sensor based on the Bis(2,4,7,8,9-pentamethyldipyrrolylmethene-3-yl)methane. J Fluoresc 24:13–17
32. Mahato P, Saha S, Das P, Agarwal H, Das A (2014) An overview of the recent developments on Hg2 + recognition. RSC Adv. https://doi.org/10.1039/C4RA03594A
33. Fegade U, Saini A, Sahoo SK, Singh N, Bendre R, Kuwar A (2014) 2,2'-(Hydrazine-1,2-diylidenedimethylylidene) bis(6-isopropyl-3-methylphenol) based selective dual-channel chemosensor for Cu2 + in semiaqueous media. RSC Adv 4: 39639–39644
34. Patil R, Moirangthem A, Butcher R, Singh N, Basu A, Tayade K, Fegade U, Hundiwale D (2014) Anil Kuwar, Al^{3+} selective colorimetric and fluorescent red shifting chemosensor: application in living cell imaging. Dalton Trans 43:2895–2899
35. Ye Z, Xiao Y, Song B, Yuan J (2014) Design and synthesis of a new terbium complex-based luminescent probe for time-resolved luminescence sensing of zinc ions. J Fluoresc 24:1537–1544
36. Safin DA, Babashkina MG, Garcia Y (2013) Crown ether-containing Schiff base as a highly efficient "turn-on" fluorescent sensor for determination and separation of Zn2+ in water. Dalton Trans 42:1969–1972
37. Li P, Zhou X, Huang R, Yang L, Tang X, Dou W, Zhao Q, Liu W (2014) A highly fluorescent chemosensor for Zn^{2+} and the recognition research on distinguishing Zn^{2+} from Cd^{2+}. Dalton Trans 43:706–713
38. Patil S, Patil R, Fegade U, Bondhopadhyay B, Pete U, Sahoo SK, Singh N, Basu A, Bendre R, Kuwar A (2015) A novel phthalazine based highly selective chromogenic and fluorogenic chemosensor for Co2+ in semi-aqueous medium: application in cancer cell imaging. Photochem Photobiol Sci 14:439–443
39. Fegade U, Sahoo SK, Attarde S, Singh N (2014) Anil Kuwar, Colorimetric and fluorescent "On-Off" chemosensor for Cu2+ in semi-aqueous medium. Sensors Actuators B 202:924–928
40. Li M-M, Huang S-Y, Ye H, Ge F, Miao J-Y, Zhao B-X (2013) A new pyrazoline-based fluorescent probe for Cu2+ in live cells. J Fluoresc 23:799–806
41. Liu S, Zhang L, Gao J, Zhou J (2013) Synthesis and analytical application of a novel fluorescent Hg2+ Probe 3′, 6′-Bis(Diethylamino)-2-((2,4-Dimethoxybenzylidene) Amino)Spiro[Isoindoline-1,9′-Xanthene]-3-Thione. J Fluoresc 23:989–996
42. Zhang D, Wang M, Wang C, Li M, Ye Y, Zhao Y (2013) Two highly sensitive and selective colorimetric "Off-On" rhodamine-based fluorescent chemosensor for Hg(II) in aqueous media. J Fluoresc 23:1045–1052
43. Kim HN, Ren WX, Kim JS, Yoon J (2012) Fluorescent and colorimetric sensors for detection of lead, cadmium, and mercury ions. Chem Soc Rev 41:3210–3244
44. The European Parliament and the Council of the European Union. Directive on the restriction of the use of certain hazardous substances in electrical and electronic equipment, 2002/95/EC
45. de Vries W (2007) Ro¨ mkens and G. Schu¨ tze. Rev Environ Contam Toxicol 191:91
46. World Health Organization (2004) Guidelines for drinking-water quality (3rd ed) vol 1, Geneva, 188
47. Fu Y, Mu L, Zeng X, Zhao J-L, Redshaw C, Ni X-L, Yamato T (2013) An NBD-armed thiacalix[4]arene-derived colorimetric and fluorometric chemosensor for Ag+: a metal–ligand receptor of anions. Dalton Trans 42:3552–3560
48. Li M, Zhang D, Liu Y, Ding P, Ye Y, Zhao Y (2014) A Novel Colorimetric and Off–On Fluorescent Chemosensor for Cr3 + in Aqueous Solution and its Application in Live Cell Imaging. J Fluoresc 24:119–127
49. Huang S, Du P, Min C, Liao Y, Sun H, Jiang Y (2013) Poly(1-amino-5-chloroanthraquinone): Highly Selective and Ultrasensitive Fluorescent Chemosensor For Ferric Ion. J Fluoresc 23:621–627
50. Shu-Yan Jiao, Ling-Ling Peng, Kun Li, Yong-Mei Xie, Mei-Zhen Ao, Xin Wang, Xiao-Qi Yu (2013) A BINOL-based ratiometric fluorescent sensor for Zn^{2+} and in situ generated ensemble for selective recognition of histidine in aqueous solution, Analyst, 138, 5762–5768
51. Ganguly A, Paul BK, Ghosh S, Kar S, Guchhait N (2013) Selective fluorescence sensing of Cu(II) and Zn(II) using a new Schiff base-derived model compound: naked eye detection and spectral deciphering of the mechanism of sensory action. Analyst 138:6532–6541

52. Choi JY, Kim G-H, Guo Z, Lee HY, Swamy KMK (2013) Jaeyoung Pai, Seunghoon Shin, Injae Shin, Juyoung Yoon, Highly selective ratiometric fluorescent probe for Au^{3+} and its application to bioimaging. Biosensors Bioelectronics 49:438–441
53. Singh AP, Murale DP, Ha Y, Liew H, Lee KM, Segev A, Suh Y-H, Churchill DG (2013) A novel, selective, and extremely responsive thienyl based dual fluorogenic probe for tandem superoxide and Hg2+ chemosensing. Dalton Trans 42:3285–3290
54. Vandana Bhalla V, Vij R, Tejpal G, Singh, Kumar M (2013) Solvent dependent competition between fluorescence resonance energy transfer and through bond energy transfer in rhodamine appended hexaphenylbenzene derivatives for sensing of Hg^{2+} ions. Dalton Trans 42:4456–4463
55. Jiangli F, Zhan P, Wen MH, Tang SJ, Wang J, Sun S, Song F, Peng X (2013) A fluorescent ratiometric chemodosimeter for Cu^{2+} based on TBET and its application in living cells. Org Lett 15(3): 492–495
56. Goswami S, Manna A, Maity AK, Paul S, Das AK, Das MK, Saha P, Quahc CK, Func H-K (2013) Selective detection and bioimaging of Pd2+ with novel 'C–CN' bond cleavage of cyano-rhodamine, cyanation with diaminomaleonitrile. Dalton Trans 42:12844–12848
57. Nouri H, Cadiou C, Lawson-Daku LM, Hauser A, Chevreux S, Déchamps-Olivier I, Lachaud F, Ternane R, Trabelsi-Ayadi M, Chuburua F, Lemercier G (2013) A modified cyclen azaxanthone ligand as a new fluorescent probe for Zn2+. Dalton Trans 42: 12157–12164
58. Sikdar A, Roy S, Haldar K, Sarkar S, Panja SS (2013) Rhodamine-based Cu2+ selective fluorosensor: synthesis, mechanism, and application in living cells. J Fluoresc 23:495–501
59. Chung PK, Liu S-R, Wang H-F, Wu S-P (2013) A pyrene-based highly selective turn-on fluorescent chemosensor for Iron(III) ions and its application in living cell imaging. J Fluoresc 23:1139–1145
60. Wang J, Chu Q, Liu X, Wesdemiotis C, Pang Y (2013) Large fluorescence response by alcohol from a Bis(benzoxazole) – Zinc(II) complex: the role of excited state intramolecular proton transfer. J Phys Chem B 117:4127–4133
61. Tan Y, Gao J, Yu J, Wang Z, Cui YuY, Yang Qian G (2013) A newfluorescent probe for distinguishing Zn2+ and Cd2+ with high sensitivity and selectivity. Dalton Trans 42:11465–11470
62. Ge F, Ye H, Luo J-Z, Wang S, Sun Y-J, Zhao B-X, Miao J-Y (2013) A new fluorescent and colorimetric chemosensor for Cu(II) based on rhodamine hydrazone and ferrocene unit. Sensors Actuators B Chemical 181:215–220
63. Har Mohindra Chawla (2013) Preeti Goel, Richa Shukla, new calix[4]arene based oxalylamido receptors for recognition of copper(II). Tetrahedron Lett 54:2766–2769
64. Kuwar A, Fegade U, Tayade K, Patil U, Puschmann H, Gite V, Dalal D, Bendre R (2013) Bis(2-Hydroxy-3-Isopropyl-6-Methyl-Benzaldehyde) Ethylenediamine: A novel cation sensor. J Fluoresc 23:859–864
65. Fangzhi Hu, Zheng B, Wang D, Liu M, Du J, Xiao D (2014) A novel dual-switch fluorescent probe for Cr(III) ion based on PET–FRET processes. Analyst 139:3607–3613
66. Chereddy NR, Niladri Raju MV, Nagaraju P, Krishnaswamy VR, Korrapati PS, Bangal PR, Rao VJ (2014) A naphthalimide based PET probe with Fe3+ selective detection ability: theoretical and experimental study. Analyst 139:6352–6356
67. Mikata Y, Nodomi Y, Kizu A, Konno H (2014) Quinoline-attached triazacyclononane (TACN) derivatives as fluorescent zinc sensors. Dalton Trans 43:1684–1690
68. Li Y, Wu J, Jin X, Wang J, Han S, Wu W, Xu J, Liu W, Yao X, Tang Yu (2014) A bimodal multianalyte simple molecule chemosensor for Mg^{2+}, Zn^{2+}, and Co^{2+}. Dalton Trans 43:1881–1887
69. Hu JH, Li JB, Qi J, Chen JJ (2015) Highly selective and effective mercury(II) fluorescent sensors. New J Chem 39:843–848
70. Fegade U, Sahoo SK, Attarde S, Singh N (2014) Anil Kuwar, Colorimetric and fluorescent "On-Off" chemosensor for Cu2+ in semi-aqueous medium. Sensors Actuators B 202:924–928
71. Hava Ozay R, Kagit M, Yildirim S, Yesilot O, Ozay (2014) Novel hexapodal triazole linked to a cyclophosphazene core rhodamine-based chemosensor for selective determination of Hg^{2+} ions. J Fluoresc 24:1593–1601
72. Liang L, Zhao L, Zeng X (2014) A highly selective turn-on fluorescent chemodosimeter for Cu^{2+} through a Cu^{2+} promoted redox reaction. J Fluoresc 24:1671–1677
73. Nayan R, Pramanik HAR, Paul PC, Singh ST (2014) A sensitive schiff-base fluorescent chemosensor for the selective detection of Zn2+. J Fluoresc 24:1099–1106
74. Li LQ, Yuan L, Liu ZH (2014) A highly selective turn on fluorescence sensor for Hg^{2+} based on rhodamine derivative. J Fluoresc 24:1357–1361
75. Patil S, Fegade U, Sahoo SK, Singh A, Marek J, Singh N, Bendre R, Kuwar A (2014) Highly sensitive ratiometric chemosensor for selective 'Naked-Eye' nanomolar detection of Co2+ in semi-aqueous media. Chemphyschem 5:2230–2235. https://doi.org/10.1002/cphc.201402076
76. Dong Z, Le X, Zhou P, Dong C, Ma J (2014) An ''off–on–off'' fluorescent probe for the sequential detection of Zn2+ and hydrogen sulfide in aqueous solution. New J Chem 38:1802–1808
77. Zhang YM, Qu WJ, Gao GY, Shi BB, Wu GY, Wei TB, Lin Q, Yao H (2014) A highly selective dual-channel chemosensor for mercury ions: utilization of the mechanism of intramolecular charge transfer blocking. New J Chem 38:5075–5080
78. Tan Y, Liu M, Gao J, Yu J, Cui Y, Yang Yu, Qian G (2014) A newfluorescent probe for Zn2+ with red emission and its application in bioimaging. Dalton Trans 43:8048–8053
79. Fegade U, Sharma H, Bondhopadhyay B, Basu A, Attarde S, Singh N, Kuwar A (2014) Turn-on" fluorescent dipodal chemosensor for nano-molar detection of Zn2+: Application in living cells imaging. Talanta 125:418–424
80. Wang M, Liu X, Lu H, Wang H, Qin Z (2015) Highly selective and reversible chemosensor for Pd2 + detected by fluorescence, colorimetry, and paper T. ACS Appl Mater Interfaces 7:1284–1289
81. Gui S, Huang Y, Hu F, Jin Y, Zhang G, Yan L, Zhang D, Zhao R (2015) Fluorescence turn-on chemosensor for highly selective and sensitive detection and bioimaging of Al3 + in living cells based on ion-induced aggregation. Anal Chem 87(3):1470–1474
82. Manna AKumarMSaikatK, Maiti K, Mondal S, Maji R, Mandal D (2015) Sukhendu Mandal, Md. Raihan Uddin, Shyamaprosad Goswami, Ching Kheng Quahd, Hoong-Kun Fund, An azodye–rhodamine-based fluorescent and colorimetric probe specific for the detection of Pd2 + in aqueous ethanolic solution: synthesis, XRD characterization, computational studies and imaging in live cells. Analyst 140:1229–1236
83. Ghorai A, Chandra Mondal J, Goutam R, Patra K (2015) A reversible fluorescent-colorimetric imino-pyridyl bis-Schiff base sensor for expeditious detection of Al3 + and HSO3 – in aqueous media. Dalton Trans 44:13261–13271
84. Zhang Z, Sha C, Liu A, Zhang Z, Xu D (2015) Highly selective detection of Cr(VI) in WaterMatrix by a simple 1,8-Naphthalimide-based turn-on fluorescent sensor. J Fluoresc 25: 335–340
85. Wu Y-C, Jiang K, Luo S-H, Cao L, Wu H-Q (2019) Zhao-YangWang, Novel dual-functional fluorescent sensors based on bis(5,6-dimethylbenzimidazole) derivatives for distinguishing of Ag + and Fe3 + in semi-aqueous medium. Spectrochim Acta Part A Mol Biomol Spectrosc 206:632–641

86. Bhosale J, Fegade U, Bondhopadhyay B, Kaur S, Singh N, Basu A, Dabur R, Bendre R, Kuwar A (2015) Pyrrole-coupled salicylimine-based fluorescence "turn on" probe for highly selective recognition of Zn2 + ions in mixed aqueous media: Application in living cell imaging. J Mol Recognit 28:369–375
87. Patil S, Patil R, Fegade U, Bondhopadhyay B, Pete U, Sahoo SK, Singh N, Basu A (2015) Ratnamala Bendre and Anil Kuwar, A novel phthalazine based highly selective chromogenic and fluorogenic chemosensor for Co2 + in semi-aqueous medium: application in cancer cell imaging. Photochem Photobiol Sci 14: 439–443
88. Patil R, Fegade U, Kaur R, Sahoo SK (2015) Narinder Singh & Anil Kuwar, Highly sensitive and selective determination of Hg2 + by using 3-((2-(1H-benzo[d]imidazol-2-yl)phenylimino)methyl)benzene-1,2-diol as fluorescent chemosensor and its application in real water sample. Supramol Chem 27:527–532
89. Pawar S, Fegade U, Bhardwaj VK, Singh N, Bendre R, Kuwar A (2015) 2-((E)-(2-aminophenylimino)methyl)-6-isopropyl-3-methylphenol based fluorescent receptor for dual Ni2 + and Cu2 + recognition: Nanomolar detection. Polyhedron 87:79–85
90. Fegade UA, Sahoo SK, Singh A, Singh N, Attarde SB, Kuwar AS (2015) A chemosensor showing discriminating fluorescent response for highly selective and nanomolar detection of Cu2 + and Zn2 + and its application in molecular logic gate. Anal Chim Acta 872:63–69
91. Zhou D, Sun C, Chen C, Cui X, Li W (2015) Research of a highly selective fluorescent chemosensor for aluminum(III) ions based on photoinduced electron transfer. J Mol Struct 1079:315–320
92. Cui J, Li D-P, Shen S-L, Liu J-T, Zhao B-X (2015) A simple and effective fluorescent probe based on rhodamine B for determining Pd2 + ions in aqueous solution. RSC Adv 5:3875–3880
93. Shengli Hu, Song J, Wua G, Cheng C, Gao Q (2015) A new pyrazoline-based fluorescent sensor for Al3 + in aqueous solution. Spectrochim Acta Part A Mol Biomol Spectrosc 136:1188–1194
94. Li L, Liu Z (2015) A colorimetric and fluorescent turn on chemodosimeter for Pd2 + detection. Spectrochim Acta Part A Mol Biomol Spectrosc 138:954–957
95. Gupta VK, Mergu N, Kumawat LK, Singh AK (2015) A reversible fluorescence "off-on-off" sensor for sequential detection of Aluminum and Acetate/Fluoride ions. Talanta 144:80–89
96. Affrose A, Parveen DS, Kumar BS, Pitchumani K (2015) Selective sensing of silver ion using berberine, a naturally occurring plant alkaloid. Sensors Actuators B 206:170–175
97. Kao M-H, Chen T-Y, Cai Y-R, Hu C-H, Liu Y-W, Jhong Y, Wu A-T (2016) A turn-on Schiff-base fluorescence sensor for Mg2þ ion and its practical application. J Lumin 169:156–160
98. Bekhradnia A, Domehri E, Khosravi M (2016) Novel coumarin-based fluorescent probe for selective detection of Cu(II). Spectrochim Acta Part A Mol Biomol Spectrosc 152:18–22
99. Sahana S, Bose S, Mukhopadhyay SK, Bharadwaj PK (2016) A highly selective and sensitive turn-on fluorescence chemosensor based on a rhodamine–adenine conjugate for Al3 + in aqueous medium: Bioimaging and DFT studies. J Lumin 169:334–341
100. Zheng X, Lee KH, Liu H, Park S-Y, Yoon SS, Lee JY, Kim Y-G (2016) A bis(pyridine-2-ylmethyl)amine-based selective and sensitive colorimetric and fluorescent chemosensor for Cu2+. Sensors Actuators B 222:28–34
101. Huang Q, Zhang Q, Wang E, Zhou Y, Qiao H, Pang L, Yu F (2016) A new ''off–on'' fluorescent probe for Al3 + in aqueous solution based on rhodamine B and its application to bioimaging. Spectrochim Acta Part A Mol Biomol Spectrosc 152:70–76
102. An R, Zhang D, Chen Y, Cui Y-z (2016) A "turn-on" fluorescent and colorimetric sensor for selective detection of Cu2 + in aqueous media and living cells. Sensors Actuators B 222:48–54
103. Wang E, Zhou Y, Huang Q, Pang L, Qiao H, Yu F, Gao B, Zhang J, Min Y, Ma T (2016) 5-Hydroxymethylfurfural modified rhodamine B dual-function derivative: Highly sensitive and selective optical detection of pH and Cu2+. Spectrochim Acta Part A Mol Biomol Spectrosc 152:327–335
104. Qin J-C, Cheng Xiao-ying, Fang R, Wang M-f, Yang Z-y, Li T-r, Li Y (2016) Two Schiff-base fluorescent sensors for selective sensing of aluminum (III): Experimental and computational studies. Spectrochim Acta Part A Mol Biomol Spectrosc 152:352–357
105. Gupta VK, Singh AK, Kumawat LK, Mergu N (2016) An easily accessible switch-on optical chemosensor for the detection of noxious metal ions Ni(II), Zn(II), Fe(III) and UO2(II). Sensors Actuators B 222:468–482
106. Kim H-S, Angupillai S, Son Y-A (2016) A dual chemosensor for both Cu2 + and Al3+: A potential Cu2 + and Al3 + switched YES logic function with an INHIBIT logic gate and a novel solid sensor for detection and extraction of Al3 + ions from aqueous solution. Sensors Actuators B 222:447–458
107. Ponnuvel K, Padmini V, Sribalan R (2016) A new tetrazole based turn-on fluorescence chemosensor for Zn2 + ions and its application in bioimaging. Sensors Actuators B 222:605–611
108. Geng J, Liu Y, Li J, Yin G, Huang W, Wang R, Quan Y (2016) A ratiometric fluorescent probe for ferric ion based on a 2,2,-bithiazole derivative and its biological applications. Sensors Actuators B 222:612–617
109. Panda U, Roy S, Mallick D, Layek A, Ray PP, Sinh C (2017) Aggregation induced emission enhancement (AIEE) of fluorenyl appended Schiff base: A turn on fluorescent probe for Al3+, and its photovoltaic effect. J Lumin 181:56–62
110. Singh DP, Dwivedi R, Singh AK, Koch B, Singh P (2017) Vinod Prasad Singh, A dihydrazone based "turn–on" fluorescent probe for selective determination of Al3 + ions in aqueous ethanol. Sensors Actuators B 238:128–137
111. Gharami S, Sarkar D, Ghosh P, Acharyya S, Aich K, Murmu N, Mondal TK (2017) A coumarin based azo-phenol ligand as efficient fluorescent "OFF-ON-OFF" chemosensor for sequential detection of Mg2 + and F–: Application in live cell imaging and as molecular logic gate. Sensors Actuators B 253:317–325
112. Lui Y, Hu J, Teng Q, Zhang H (2017) Ferrocenyl-based thioethers and sulphones as optical, and electrochemical sensors for the differential detection of Hg2 + and Cu2 + ions. Sensors Actuators B 238:166–174
113. Liu J, Qian Y (2017) A novel pyridylvinyl naphthalimide-rhodamine dye: synthesis, naked-eye visible and ratiometric chemodosimeter for Hg2+/Fe3+. J Lumin 187:33–39
114. Gao Y, Zhang C, Peng S, Chen H (2017) A fluorescent and colorimetric probe enables simultaneous differential detection of Hg2 + and Cu2 + by two different mechanisms. Sensors Actuators B 238:455–461
115. Maniyazagan M, Mariadasse R, Jeyakanthan J, Lokanath NK, Naveen S, Premkumar K, Muthuraja P, Manisankar P, Stalin T (2017) Rhodamine based "turn–on" molecular switch FRET–sensor for cadmium and sulfide ions and live cell imaging study. Sensors Actuators B 238:565–577
116. Dong W-K, Akogun SF, Zhang Y, Sun Y-X, Dong X-Y (2017) A reversible "turn-on" fluorescent sensor for selective detection of Zn2+. Sensors Actuators B 238:723–734
117. Ghosh U, Bag SS, Mukherjee C (2017) Bis-pyridobenzene as a fluorescence light-up sensor for Hg2 + Ion in water. Sensors Actuators B 238:903–907
118. Li H, Wang J, Zhang ShuJiang, Gong ChenLiang, Wang F (2018) A novel off-on fluorescent chemosensor for Al3 + derived from a 4,5-diazafluorene Schiff base derivative. RSC Adv 8:31889–31894
119. Shuai Wang H, Ding Y, Wang C, Tu FY, Liu G, Pu S (2018) An ''off–on–off'' sensor for sequential detection of Cu2 + and

hydrogen sulfide based on a naphthalimide–rhodamine B derivative and its application in dual-channel cell imaging. RSC Adv 8: 33121–33128

120. Xu K, Li Y, Si Y, He Y, Ma J, He J, Hou H, Li K (2018) A "turn-on" fluorescent chemosensor for the detection of Hg(II) in buffer free aqueous solution with excellent selectivity. J Lumin 204:182–188

121. Rui Y, Wang Z, Du Z, Wang H, Cheng Xu, Xiong J (2018) A biomimetic fluorescent chemosensor for highly sensitive zinc(II) detection and its application for cell imaging. RSC Adv 8:33361–33367

122. Meng X, Cao D, Hu Z, Han X, Li Z, Ma W (2018) A highly sensitive and selective chemosensor for Pb2 + based on quinoline–coumarin. RSC Adv 8:33947–33951

123. Kumar GGangatharanV, Kesavan MP, Tamilselvi A, Rajagopal G, Raja JD, Sakthipandi K, Rajesh J, Sivaraman G (2018) A reversible fluorescent chemosensor for the rapid detection of Hg2 + in an aqueous solution: Its logic gates behavior. Sensors Actuators B Chem 273:305–315

124. Khanra S, Ta S, Ghosh M, Chatterjee S, Das D (2019) Subtle structural variation in azine/imine derivatives controls Zn2 + sensitivity: ESIPT-CHEF combination for nano-molar detection of Zn2 + with DFT support. RSC Adv 9:21302–21310

125. Ghorai P, Banerjee S, Nag D, Mukhopadhyay SK, Saha A (2019) Design and synthesis of a novel fluorescentcolorimetric chemosensor for selective detection of Zn(II) and Cu(II) ions with applications in live cell imaging and molecular logic gate. J Lumin 205:197–209

126. Zhang Y, Zhang C, Wu Y, Zhao B, Wang L, Song B (2019) A novel water-soluble naked-eye probe with a large Stokes shift for selective optical sensing of Hg2 + and its application in water samples and living cells. RSC Adv 9:23382–23389

127. Serkan E (2019) Fluorometric dual sensing of Hg2 + and Al3 + by novel triphenylamine appended rhodamine derivative in aqueous media. Sensors Actuators B Chem 290:558–564

128. Rout K, Manna AK, Sahu M, Mondal J, Singh SK, Patra GK (2019) Triazole-based novel bis Schiff base colorimetric and fluorescent turn-on dual chemosensor for Cu2+ and Pb2+: application to living cell imaging and molecular logic gates. RSC Adv 9: 25919–25931

129. Yang Y, Yu Z, Shi W, Ma F, Li Y (2019) Colorimetric fluorescence probe detecting Hg2 + and OCl– based on intramolecular charge transfer and excited-state intramolecular roton transfer mechanisms. J Lumin 209:102–108

130. Vishaka VH, Saxena M, Geetha Balakrishna R, Latiyanbc S, Jainc S (2019) Remarkably selective biocompatible turn-on fluorescent probe for detection of Fe3 + in human blood samples and cells. RSC Adv 9:27439–27448

131. Jung JM, Yun D, Lee H, Kim K-T, Kim C (2019) Selective chemosensor capable of sensing both CN – and Zn2+: Its application to zebrafish. Sensors Actuators B Chem 297:126814

132. Zhang Y, Li H, Gao W, Pu S (2019) Dual recognition of Al3 + and Zn2 + ions by a novel probe based on diarylethene and its application. RSC Adv 9:27476–27483

133. Ganesan JS, Sepperumal M, Balasubramaniem A, Ayyanar S (2019) A novel pyrazole bearing imidazole frame as ratiometric fluorescent chemosensor for Al3+/Fe3 + ions and its application in HeLa cell imaging. Spectrochim Acta Part A :117993

134. Sutariya PG, Soni H, Gandhi SA (2019) Alok Pandya, Novel tritopic calix[4]arene CHEF-PET fluorescence paper based probe for La3+, Cu2+, and Br–: Its computational investigation and application to real samples. J Lumin 212:171–179

135. Akshay Krishna TG, Tekuri V, Mohan M, Trivedi DR (2019) Selective colorimetric chemosensor for the detection of Hg2 + and arsenite ions using Isatin based Schiff's bases; DFT Studies and applications in test strips. Sensors Actuators B Chem 284: 271–280

136. Srivastava S, Thakur N, Singh A, Shukla P, Maikhuri VK, Garg N, Prasad A, Pandey R (2019) Development of a fused imidazo[1, 2-a]pyridine based fluorescent probe for Fe3 + and Hg2 + in aqueous media and HeLa cells. RSC Adv 9:29856–29863

137. Said AI, Georgiev NI, Bojinov VB (2019) A smart chemosensor: Discriminative multidetection and various logic operations in aqueous solution at biological pH. Spectrochim Acta Part A Mol Biomol Spectrosc 223:117304

138. Berrones-Reyes JC, Munoz-FloresBM, Cant´on-Di´az AM, Treto-Su´arez MA (2019) Dayan P´aez-Hern´andez, Eduardo Schott, Ximena Zarate, Vıctor M. Jim´enez-P´erez, Quantum chemical elucidation of the turn-on luminescence mechanism in two new Schiff bases as selective chemosensors of Zn2+: synthesis, theory and bioimaging applications. RSC Adv 9:30778–30789

139. Panunzi B, Diana R, Concilio S, Sessa L, Tuzi A, Piotto S, Caruso U (2019) Fluorescence pH-dependent sensing of Zn(II) by a tripodal ligand. A comparative X-ray and DFT study. J Lumin 212: 200–206

140. Li S, Cao D, Hu Z, Li Z, Meng X, Hana X, Ma W (2019) A chemosensor with a paddle structure based on a BODIPY chromophore for sequential recognition of Cu2 + and HSO3-. RSC Adv 9:34652–34657

141. Gu Y-Q, Shen W-Y, Mi Y, Jing Y-F, Yuan J-M, Yu P, Zhuc X-M (2019) Dual-response detection of Ni2 + and Cu2 + ions by a pyrazolopyrimidine-based fluorescent sensor and the application of this sensor in bioimaging. RSC Adv 9:35671–35676

142. Xu J, Yang Y, Baigude H, Zhao H (2019) New ferrocene–triazole derivatives for multisignaling detection of Cu2 + in aqueous medium and their antibacterial activity, Spectrochimica Acta Part A :117880

143. Zhang Q, Ma R, Li Z, Liu Z (2019) A multi-responsive crown ether-based colorimetric/fluorescent chemosensor for highly selective detection of Al3+, Cu2 + and Mg2+. Spectrochim Acta Part A Mol Biomol Spectrosc 94:117857

144. Mao X, Su H, Tian D, Li H, Yang R (2013) Bipyrene-functionalized graphene as a "Turn-on" fluorescence sensor for manganese(II) ions in living cells. ACS Appl Mater Interfaces 5: 592–597

145. Guan J, Tu Q, Chen L, Yuan M-S, Wang J (2019) A benzothiazole-rhodol based luminophor: ESIPT-induced AIE and an application for detecting Fe2 + ion. Spectrochim Acta Part A Mol Biomol Spectrosc 220:117114

146. Park GJ, Na YJ, Jo HY, Lee SA, Kim C (2014) A colorimetric organic chemo-sensor for Co2 + in a fully aqueous environment. Dalton Trans 43:6618–6622

147. Cox RP, Sandanayake S, Scarborough DLA, Izgorodina EI, Langford SJ, Bell TDM (2019) Investigation of cation binding and sensing by new crown ether core substituted naphthalene diimide systems. New J Chem 43:2011–2018

148. Minoo, Bagheri, Masoomi MY (2020) Sensitive ratiometric fluorescent metal-organic framework (MOF) sensor for calcium signaling in human blood ionic concentrations media. ACS Appl Mater Interfaces 12(4):4625–4631

149. Zhou J-R, Liu D-P, He Y, Kong X-J, Zhang Z-M, Ren Y-P, Long L-S, Huang R-B, Zheng L-S (2014) Lan-Sun Zheng, A highly selective colorimetric chemosensor for cobalt(II) ions based on a tripodal amide ligand. Dalton Trans 43:11579–11586

150. Yang X, Wang Y, Liu R, Zhang Y, Tang J, Yang E-b, Zhang D, Zhao Y, Ye Y (2019) A novel ICT-based two photon and NIR fluorescent probe for labile Fe2 + detection and cell imaging in living cells. Sensors Actuators B Chem 288:217–224

151. Pendin D, Norante R, Nadai AD, Gherardi G, Vajente N, Basso E, Kaludercic N, Mammucari C, Paradisi C, Pozzan T, Mattarei A

(2019) A Synthetic Fluorescent Mitochondria-Targeted Sensor for Ratiometric Imaging of Calcium in Live Cells. Angew Chem Int Ed 58:9917–9922

152. Yang M, Chae JB, Kim C, Harrison RG (2019) A visible chemosensor based on carbohydrazide for Fe(II), Co(II) and Cu(II) in aqueous solution. Photochem Photobiol Sci 18:1249–1258

153. Huang M-X, Lv C-H, Huang Q-D, Lai J-P, Sun H (2019) A novel and fast responsive turn-on fluorescent probe for the highly selective detection of Cd2 + based on photo-induced electron transfer. RSC Adv 9:36011–36019

154. Swami S, Agarwala A, Behera D, Shrivastava R (2018) Diaminomaleonitrile based chromo-fluorescent receptor molecule for selective sensing of Mn(II) and Zn(II) ions. Sensors Actuators B Chem 260:1012–1017

155. Sargenti A, Farruggia G, Malucelli E, Cappadone C, Merolle L, Marraccini C, Andreani G, Prodi L, Zaccheroni N (2014) Massimo Sgarzi, Claudio Trombini, Marco Lombardo, Stefano Iottia, A novel fluorescent chemosensor allows the assessment of intracellular total magnesium in small samples. Analyst 139: 1201–1207

156. Zhao B, Xu Yu, Fang Y, Wang L, Deng Q (2015) Synthesis and fluorescence properties of phenanthro[9,10-d] imidazole derivative for Ag + in aqueous media. Tetrahedron Lett 56:2460–2465

157. Juhye Kang HK, Kang H, Kim J, Lee EJ, Song K-D, Jeong C, Kim J, Kim (2013) Fluorescent chemosensor based on bispicolylamine for selective detection of magnesium ions. Supramol Chem 25:65–68